

Los Alamos
NATIONAL LABORATORY
research note

Applied Physics Division, X-3
Computational Analysis and Simulation, X-3

To/MS: Distribution
From/MS: S. G. Mashnik, X-3-MCC, MS A143
Phone/FAX: 7-9946/5-4479
Email: mashnik@lanl.gov
Symbol: X-3-RN(U)09-09, LA-UR-09-04324
Date: June 30, 2009

**FY2009 Upgrade and Validation of CEM03.02(03) and
LAQGSM03.03 for MCNP6, MCNPX, and MARS15**
(by S. G. Mashnk, K. K. Gudima, A. J. Sierk, and N. V. Mokhov)

Abstract

This Research Note presents a summary and progress report on the fiscal year 2009 upgrade of CEM03.02(03) and LAQGSM03.03 event-generators for the transport codes MCNP6, MCNPX, and MARS15 and on their validation and testing against a large variety of recent measurements. Part of the work described here was performed by Dr. K. K. Gudima at the Institute of Applied Physics (IAP), Academy of Science of Moldova with a help from Dr. M. I. Baznat (IAP) in collaboration with S. G. Mashnik of X-3-MCC (LANL) and N. V. Mokhov of FNAL. Another part was performed by S. G. Mashnik and A. J. Sierk (T-2) in collaboration with K. K. Gudima, in consultation with and with support from N. V. Mokhov and R. E. Prael (X-3-MCC).

1. Introduction

During the last decade, for a number of applications like Accelerator Transmutation of nuclear Wastes (ATW), Accelerator Production of Tritium (APT), the Spallation Neutron Source (SNS), the Facility for Rare Isotope Beams (FRIB), Proton Radiography (PRAD) as a probe for the Advanced Hydro-test Facility, astrophysical work for NASA, and other projects, we have developed at the Los Alamos National Laboratory improved versions[1, 2] of the Cascade-Exciton Model (CEM) [3], to describe nucleon-, pion-, and photon-induced reactions at incident energies up to about 5 GeV and the Los Alamos version of the Quark-Gluon String Model (LAQGSM) [4, 5], to describe reactions induced by particles and nuclei at energies up to about 1 TeV/nucleon (see further references in [6]).

One of the major milestones of the Monte Carlo Codes Group (X-3-MCC) of the Applied Physics Division of LANL for the fiscal year 2009 (FY2009) is development and completion of a merged version of the MCNP5 and MCNPX transport codes, named MCNP6. Here, we present an upgrade of CEM03.02 (and CEM03.03) and LAQGSM03.03 we performed during FY2009 for

the merged MCNP6, MCNPX, and MARS15, as well as results of an extensive validation and testing of our upgraded codes against a large variety of experimental data.

2. CEM03.02(03) Upgrade

During FY2009, we were not funded to perform extensive development and improvement of CEM03.02, CEM03.03, or LAQGSM03.03. Therefore, we fixed only bugs and small errors we found in CEM03.02(03) and LAQGSM03.03 and performed the minimum necessary upgrades to avoid possible unphysical results or crashes of MCNP6, MCNPX, and MARS15 when using our event generators.

2.A. First, we observed an error in a kinematics formula of **subroutine fisgem** (in both CEM and LAQGSM), that originates from **subroutine fiss** of the Furihata code GEM2 [7] which we use with some modifications in our event generators. We corrected this error in both CEM and LAQGSM and tested how this corrections affects the results of the codes.

2.B. We found that in some very rare events (we located only three such cases from about 2×10^8 events for different reactions) of high-energy reactions, after emitting many cascade nucleons and several preequilibrium particles, we could produce a “nucleus” with $A = Z = 13$ ($N = 0$). This happens after the INC, when moving from the preequilibrium to the evaporation stage of a reaction. At this point, CEM03.02 does crash, as for $A = 13$ it does not call Fermi break-up to disintegrate this “nucleus”, but having $N = 0$ crashes the code when trying to calculate the pairing energy of such a “nucleus”. This is a typical example of a “bug” that may happen very, very rarely after a very extensive reaction described by the classical INC of CEM03.02 followed by emission of many preequilibrium nucleons. We fixed this “bug” by causing such “nuclei” to decay with the Fermi break-up model.

2.C. To avoid possible rare events producing unstable nuclides with $A \leq 13$ via a very asymmetric fission by CEM03.02, we modified slightly **subroutine fisgem** to limit the mass number of all possible fission fragments to $A > 12$. This eliminates the necessity of using the version CEM03.03, where the same problem was earlier solved in a different but more time consuming way (see details in Ref. [6]).

2.D. Finally, we corrected an error in a comment of **block data bd1** and added a few more comments in some other routines.

Sample results by CEM03.02 are shown in Figs. 1–2. The results obtained with the upgraded version of CEM03.02 are labeled as “CEM03.02, new” in the legends of the figures, while the results by the old version are labeled as “CEM03.02, old”. The results by the upgraded version are almost the same as by the old version, differing only that the upgraded version does not provide those very rare unphysical results, and would not crash MCNP6 or MCNPX. All the upgrades of CEM03.02 were also done in CEM03.03 used by MARS15, so that MARS15 should also be free of these problems.

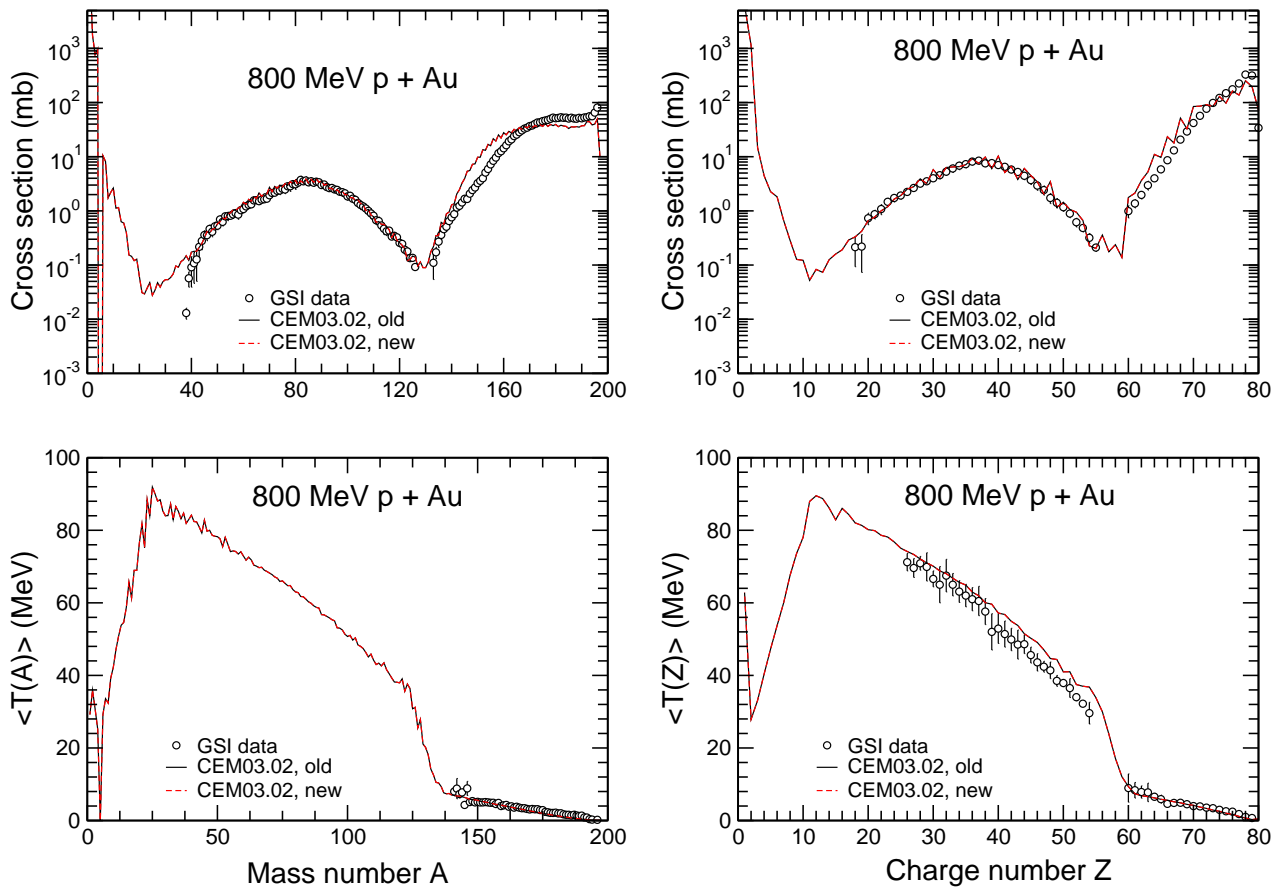


Figure 1: A - and Z -distributions of the nuclide production cross sections and of the mean kinetic energy of products from interaction of 800 MeV protons with Au calculated by the old CEM03.02 (noted as “CEM03.02, old”) and by the FY2009 upgraded version (noted as “CEM03.02, new”) compared with GSI measurements [8].

3. Validation and testing the upgraded CEM03.02(03)

We have validated the upgraded CEM03.02 and CEM03.03 against a large variety of different nuclear reaction data of interest to spallation applications by participating with both our CEM03.02 and CEM03.03 codes in the International Benchmark of Spallation Models organized during 2008–2009 by the IAEA, Vienna [10]. All calculations with CEM03.02 for this Benchmark were performed in LANL Group T-2 by A. J. Sierk with help from S. G. Mashnik, in cooperation with K. K. Gudima and M. I. Baznat, while all calculations with CEM03.03 were performed at IAP of Moldova by K. K. Gudima with help from M. I. Baznat, in cooperation with S. G. Mashnik and A. J. Sierk. We submitted our results to the organizers of the Benchmark [10] by the initial official deadline of January 31, 2009, and presented part of our results at the **Nuclear Spallation Reactions Satellite Meeting**,

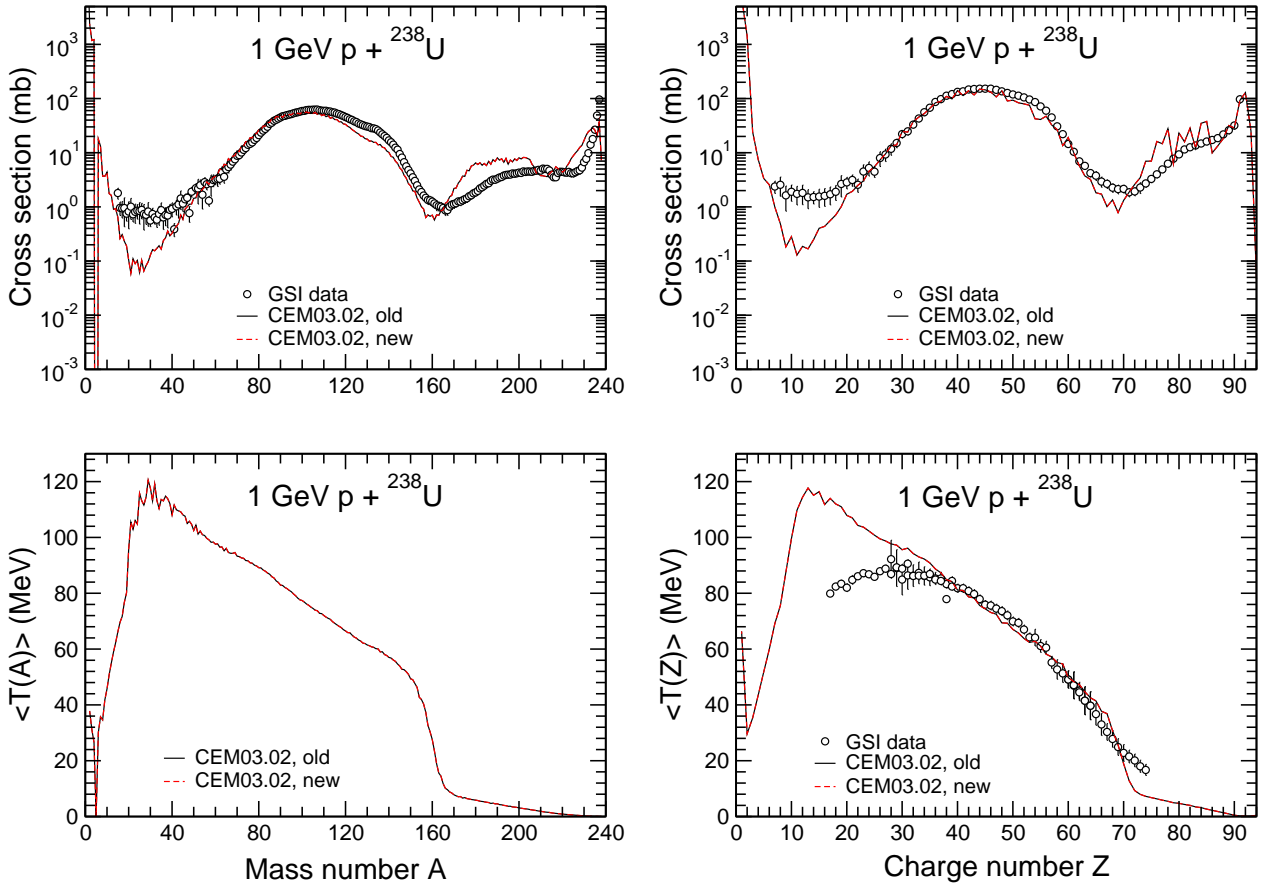


Figure 2: The same as in Fig. 1, but for $1 \text{ GeV } p + {}^{238}\text{U}$. The GSI data are from Ref. [9].

International Topical Meeting on Nuclear Research Applications and Utilization of Accelerators, 4–8 May 2009, IAEA, Vienna, Austria [11, 12].

Part of our results are shown in Figs. 3–4. From these results, as well as from many other results presented on numerous plots posted at the Benchmark web site [10], we see that CEM03.02 and CEM03.03 describe quite well most of the experimental data covered by the Benchmark. On the whole, our codes provide a better overall agreement with the data as compared with all the other codes involved in the Benchmark, especially for complex-particle spectra. This conclusion is accurate as of the end of June, 2009. After the original deadline of 31 January, 2009, a few groups asked for additional time to possibly adjust their codes and finish their calculations. A final assessment of the relative predictive capability of all the tested spallation models awaits the final presentation of all calculations.

Fig. 4 shows contributions from different reaction mechanisms to the total spectra of p and d produced at 54 degrees from 542 MeV $n + {}^{210}\text{Bi}$ reactions.

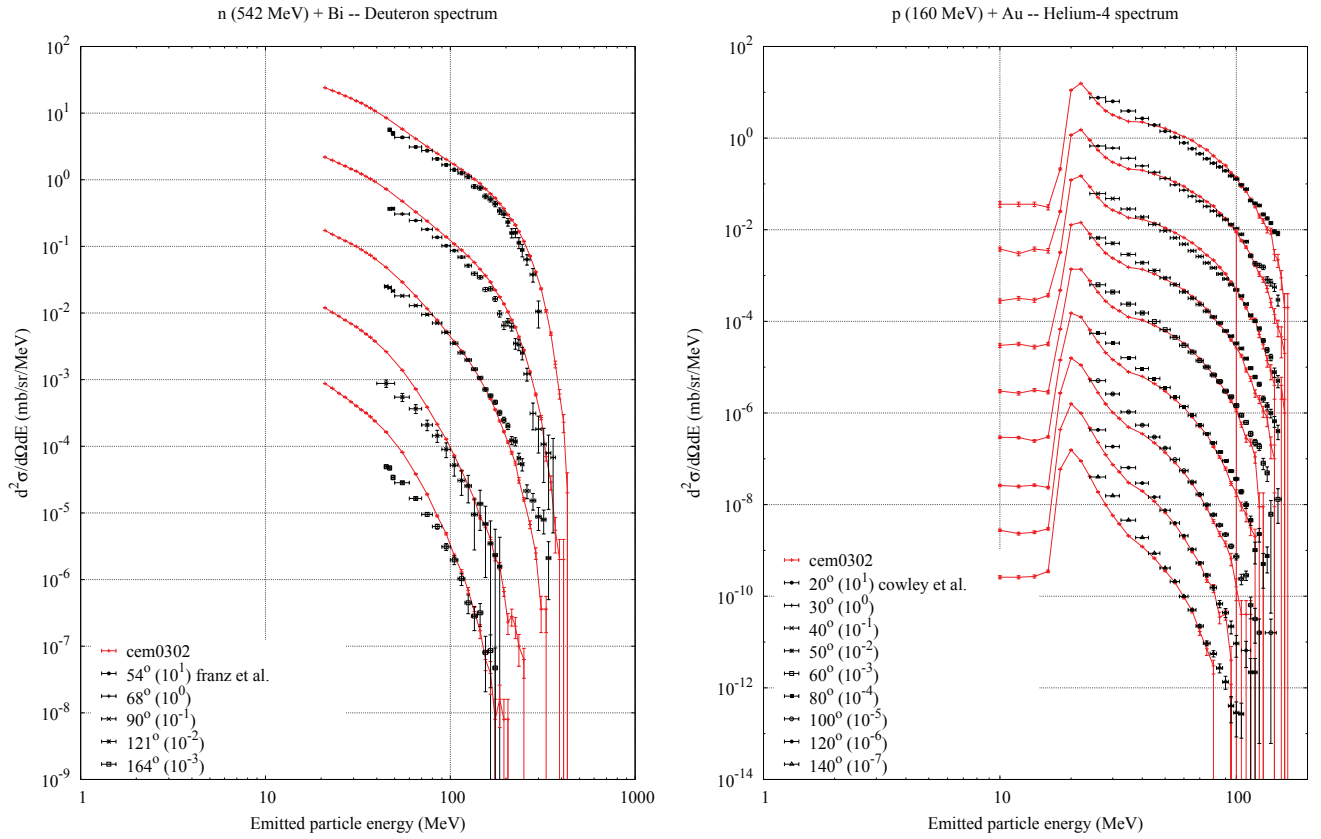


Figure 3: Experimental double-differential spectra of deuterons at 54, 68, 90, 121, and 164 degrees from 542 MeV $n + \text{Bi}$ by Franz et al. [13] and of ${}^4\text{He}$ at 20, 30, 40, 50, 60, 80, 100, 120, and 140 degrees from 160 MeV $p + {}^{197}\text{Au}$ by Cowley et al. [14] (symbols) compared with our CEM03.02 results (red lines) presented at the Benchmark [10].

Finally, we tested how our upgraded CEM03.02 describes production of delayed-neutron emitters ${}^9\text{Li}$, ${}^{16}\text{C}$, and ${}^{17}\text{N}$ from a variety of proton-induced reactions at 156, 1000, and 2800 MeV measured 45 years ago by Dostrovsky et al. [15]. This work was initiated by Bob Williams and Erik Silvertson of **Directed Technologies, Inc.** in Virginia, as a part of their complex study of a possible interrogation of different objects with protons from an accelerator in flight. They contacted us and asked to collaborate with them and to perform some calculations for their team under a “Work for Other” contact. Unfortunately, they did not send us their documents and the suggested “Work for Other” contract was not signed; therefore, we had to postpone this study until we receive the promised payment. However, some preliminary results we found (see Fig. 5) help us understand the situation with the prediction of delayed-neutron emitters by CEM03.02. ${}^9\text{Li}$, ${}^{16}\text{C}$, and ${}^{17}\text{N}$ are neutron-rich nuclides, and is quite difficult for any model to calculate their production from arbitrary nucleon-induced reactions. From Fig. 5, we see that CEM03.02 describes reasonably well their production from light and medium targets ($A < 30 - 40$), at all the energies considered here. In such reactions, these nuclides are produced mainly via

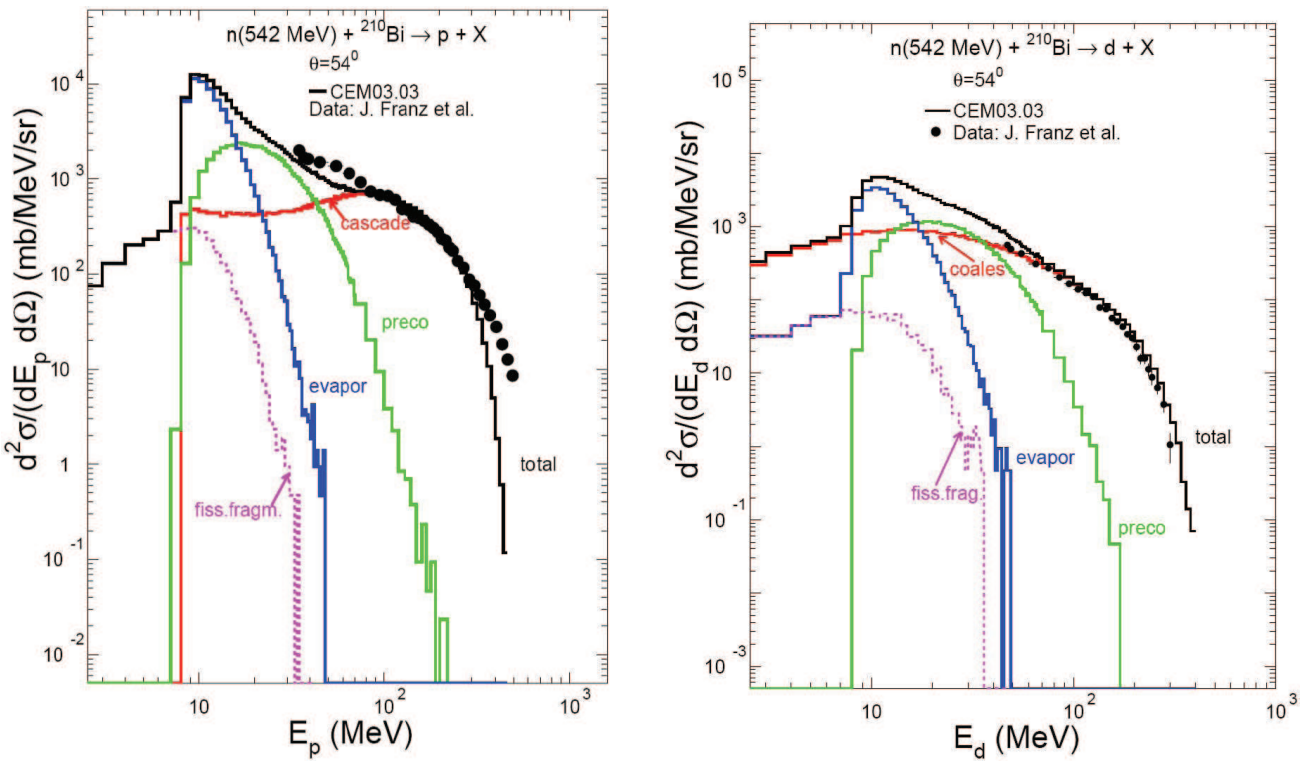


Figure 4: Experimental double-differential spectra of protons and deuterons at 54 degrees from 542 MeV $n + \text{Bi}$ (black circles) [13] compared with our results by CEM03.03 (histograms) presented at the Benchmark [10]. Contributions from intra-nuclear cascade, preequilibrium, evaporation before or without fission, coalescence, and evaporation from fission fragments to the total spectra (black histograms) are shown by different colors, as indicated.

spallation reactions as “residual nuclei” after emission of a number of nucleons, complex particles, and light fragments (and production of pions) from the target nuclei. However, for heavier targets ($A > 40$), when ${}^9\text{Li}$, ${}^{16}\text{C}$, and ${}^{17}\text{N}$ are produced mainly as emitted fragments with only a small contribution from deep-spallation reactions as “residual nuclei”, CEM03.02 describes satisfactorily only the yield of ${}^9\text{Li}$, mostly via their evaporation from compound nuclei. The yields of ${}^{16}\text{C}$ and ${}^{17}\text{N}$ from $A > 40$ nuclear targets are strongly underestimated, by a factor from 5 to 50, indicating that a further improvement and development of CEM03.02 is needed.

4. LAQGSM03.03 Upgrade

4.A. We incorporated into LAQGSM03.03 all the corrections listed above in Sections *2.A* and *2.B* as the errors we encountered in CEM03.02 which motivated these upgrades could as well occur in similarly very rare cases in LAQGSM. We modified slightly the **subroutine precol** of the file **LAQ3a.f** and the **subroutine fisgem** of the file **FROMCEM09.f** to account for these upgrades. Several results from the upgraded version (labeled as “LAQGSM03.03, new”) are

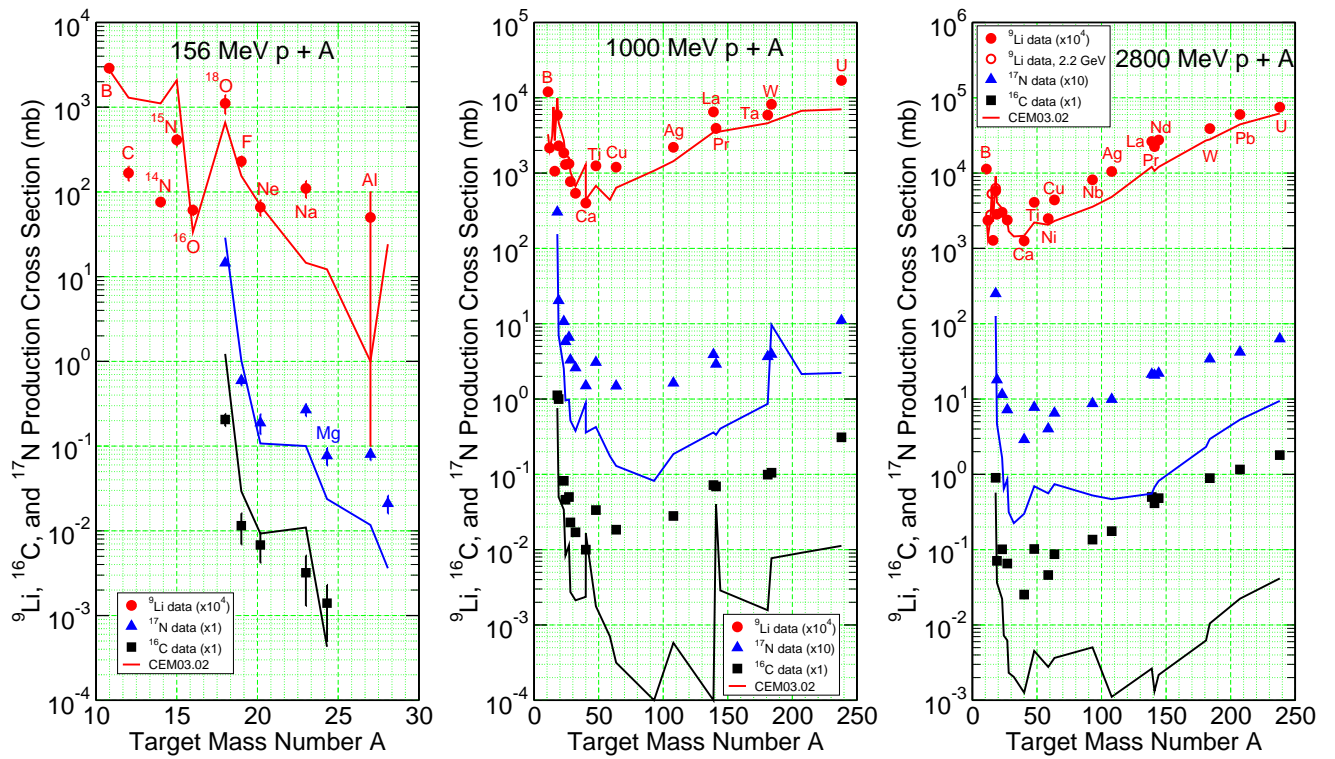


Figure 5: Cross sections for the production of delayed-neutron emitters ${}^9\text{Li}$, ${}^{16}\text{C}$, and ${}^{17}\text{N}$ from various targets for 156 MeV, 1.0 and 2.8 GeV incident protons calculated by CEM03.02 (lines) compared with experimental data by Dostrovsky et al. [15], as indicated.

compared with corresponding results from the old version (labeled as “LAQGSM03.03, old”) in Figs. 6–9.

Fig. 6 shows that results for 1 GeV $\text{p} + {}^{238}\text{U}$ reaction by the “new”, i.e. upgraded version of LAQGSM03.03 practically coincide with results the the “old” version, just as we obtained for this reaction with CEM03.02. Similar results were obtained with LAQGSM03.03 for other proton-induced reactions. However, as we can see from Figs. 7–8, the situation changes if we calculate with LAQGSM these reactions in inverse kinematics, as they were actually measured at GSI, i.e. as ${}^{238}\text{U} + \text{p}$ and ${}^{197}\text{Au} + \text{p}$. In this case, the velocity of the system where nuclear interactions occur relative to the Lab system is much higher, the kinematics transformations are more important, and we see a big difference in the mean kinetic energy of the final products: The sharp unphysical decrease of the mean kinetic energy of products in the fission region disappeared (compare the dashed red lines with the black solid ones). A smaller change between the “old” mean production angles $\langle \Theta \rangle$ calculated with the error in the kinematics and the “new” results free of that error is shown. Naturally, a similar situation should be expected when calculating fragmentation of a projectile nucleus in high-energy interactions of two heavy ions, just as proved by the results shown in Fig. 9.

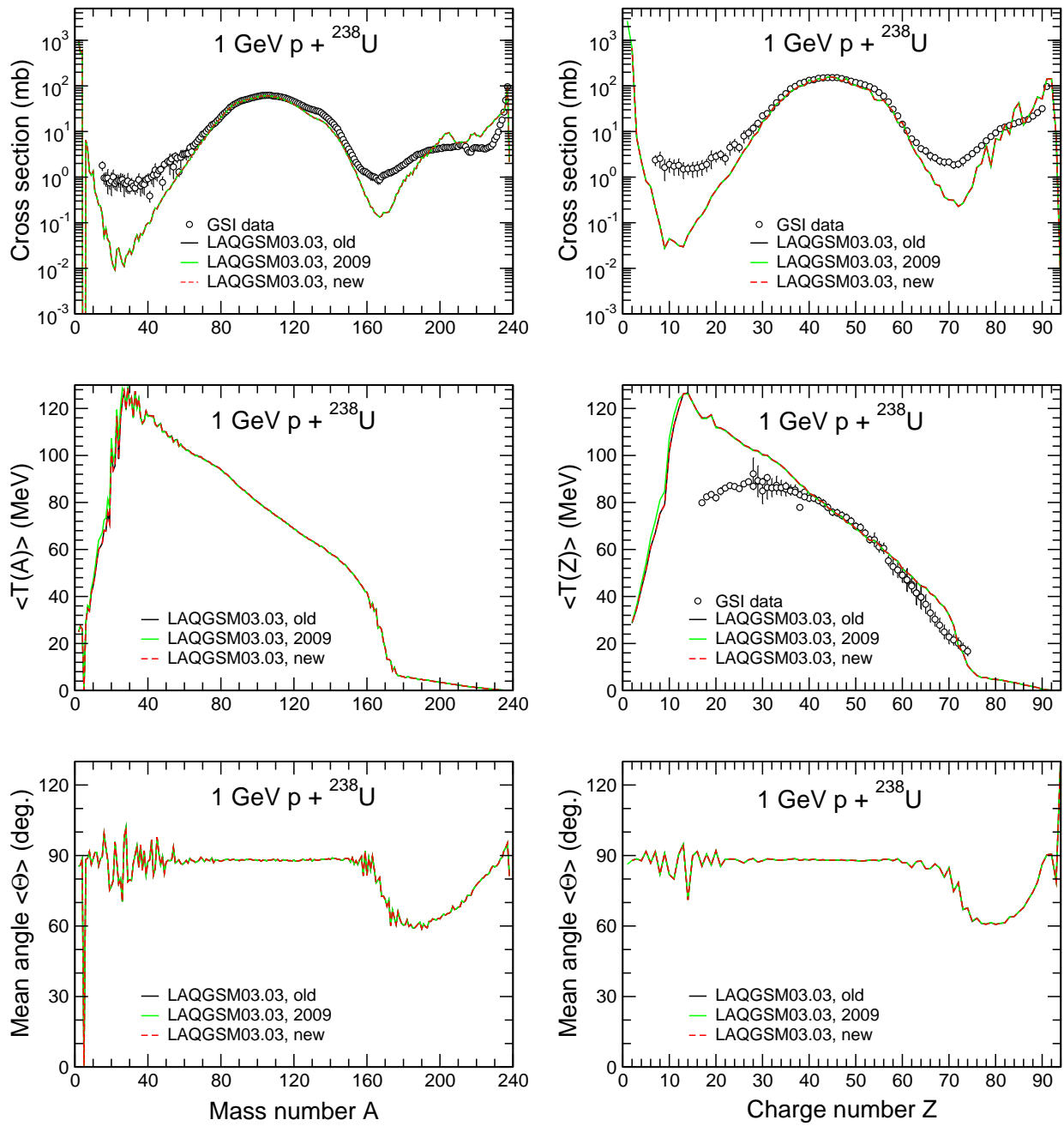


Figure 6: A- and Z-distributions of the nuclide production cross sections, mean kinetic energy of products, and mean angles of production (in the Lab system) from interaction of 1 GeV protons with ^{238}U calculated by the old LAQGSM03.03 (noted as “LAQGSM03.03, old”), by the upgraded version as described in Section 4.A (noted as “LAQGSM03.03, new”), and by the latest upgrade as described in Section 4.B (noted as “LAQGSM03.03, 2009”) compared with the GSI data [9].

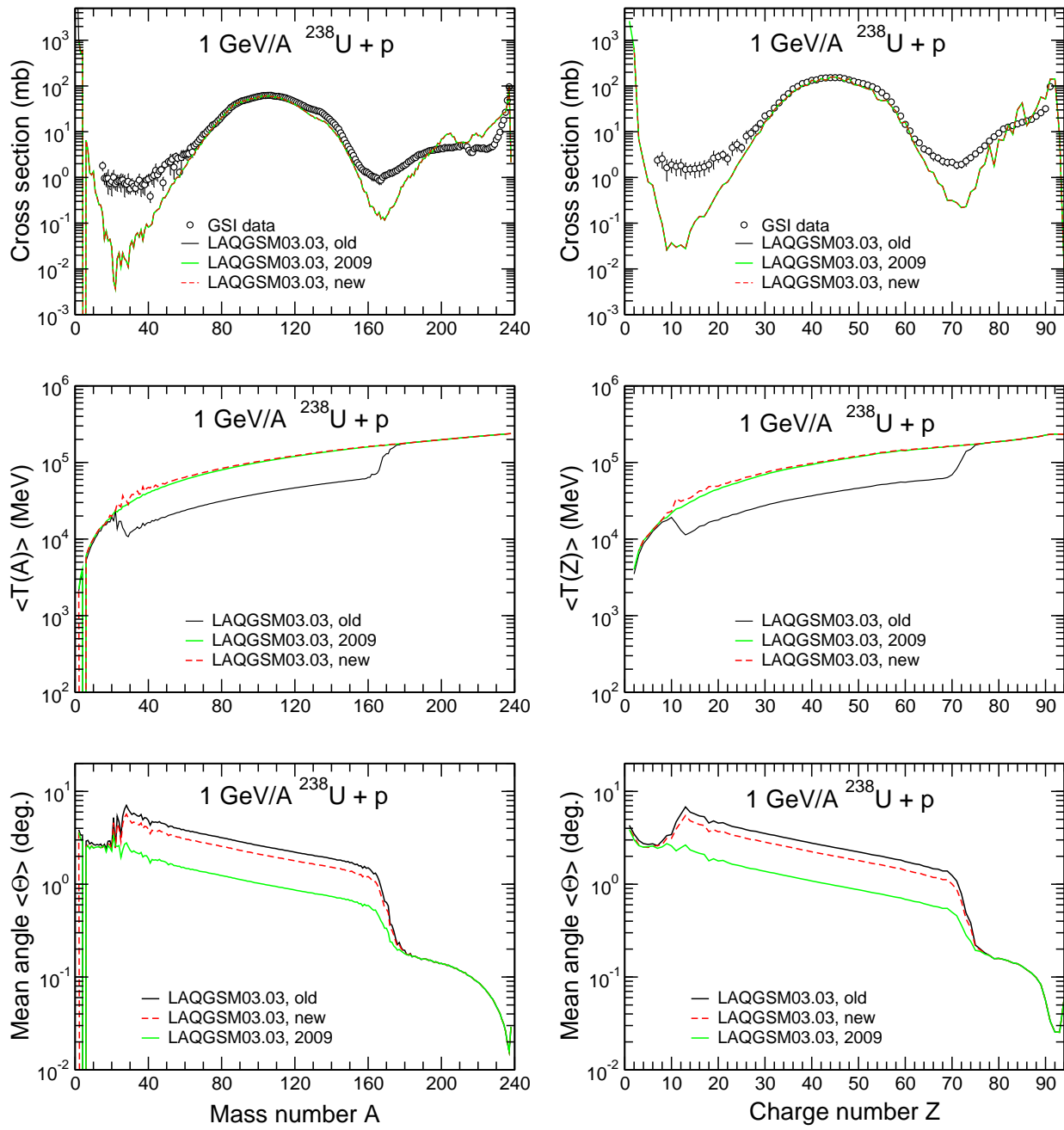


Figure 7: The same as in Fig. 6, but calculated in inverse kinematics, just as was measured at GSI, i.e., as: $^{238}\text{U} + p$.

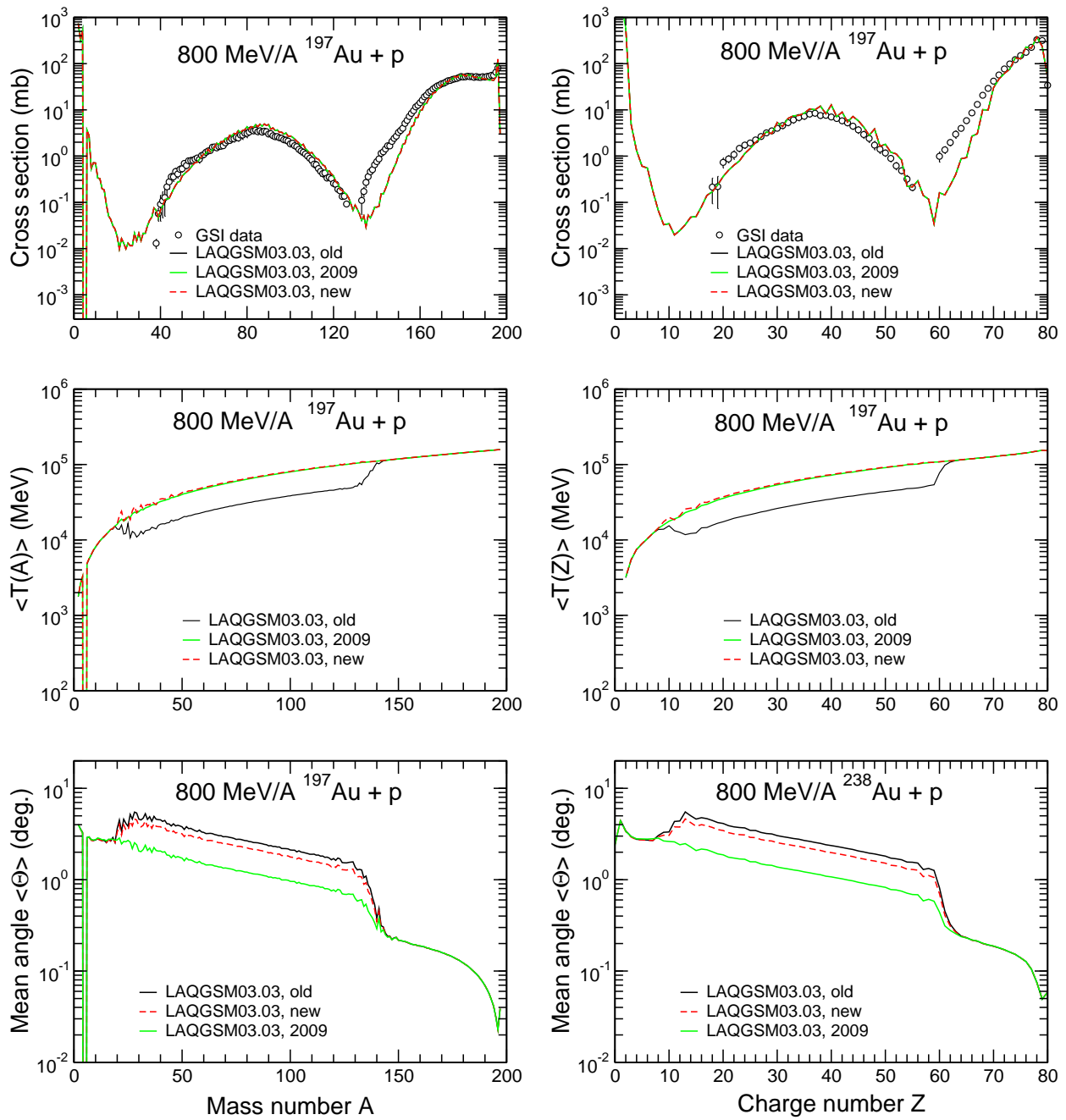


Figure 8: The same as in Fig. 7, but for 800 MeV/A $^{197}\text{Au} + \text{p}$. GSI data are from [8].

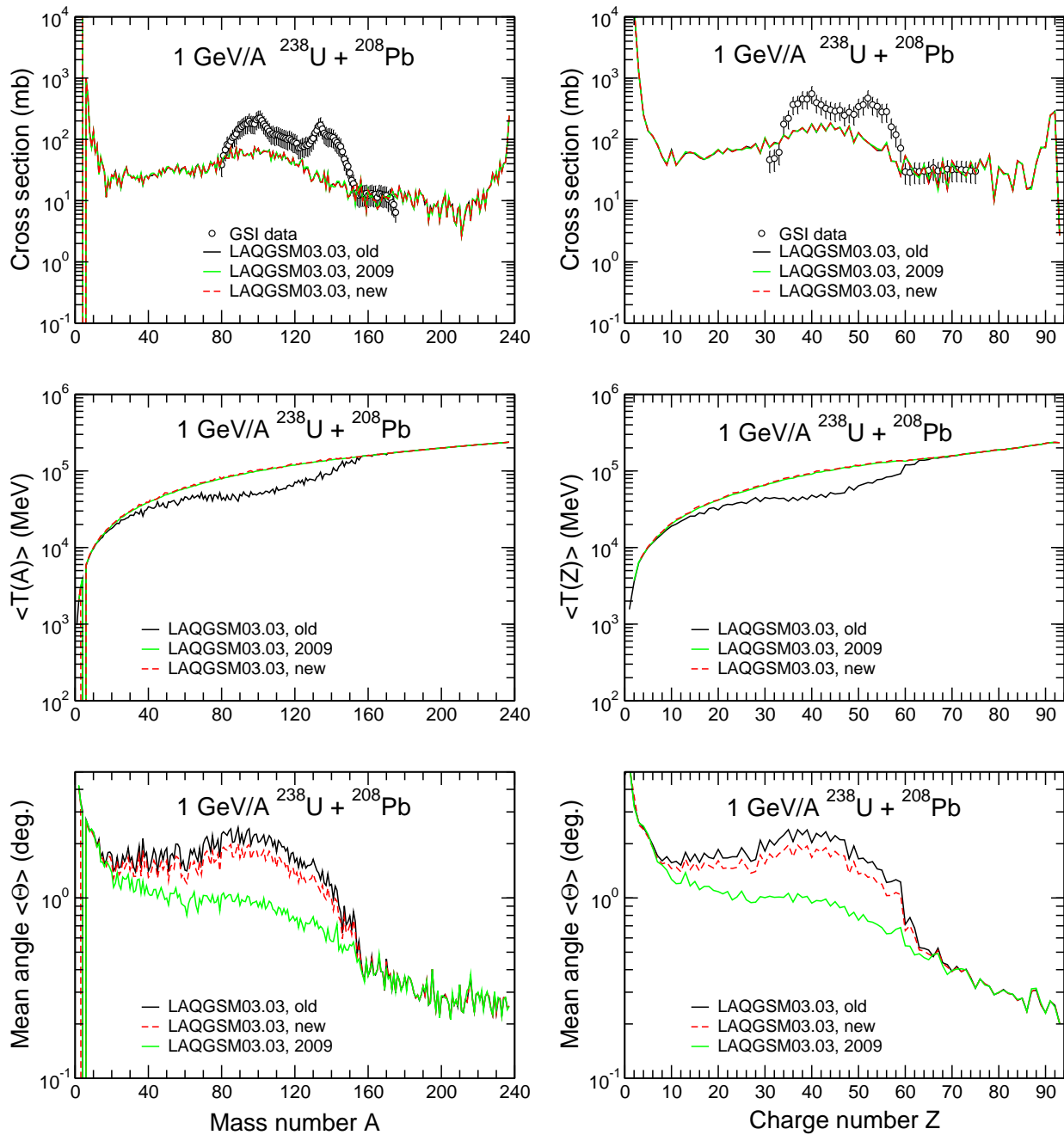


Figure 9: The same as in Fig. 7, but for interaction of two heavy ions, namely $1 \text{ GeV}/A \ ^{238}\text{U} + ^{208}\text{Pb}$. GSI data are from [16].

4.B. Even after correcting the kinematics error, some results on fragmentation of projectile nuclei in reactions induced by high-energy heavy ions look suspicious and are likely unphysical. It is difficult to understand the sudden rise of the mean angle of produced nuclei in the fission region, which occurs around $A = 28$ and $Z = 12$, just on the border of changing the mechanism of nuclide production. The heaviest fragment that can be evaporated by the Generalized-Evaporation Model GEM2 of Furihata [7] used in LAQGSM and CEM is just $^{28}_{12}\text{Mg}$; i.e., products lighter than or equal to ^{28}Mg are produced in reactions induced by heavy ions mainly as evaporated fragments, while heavier products are “residual nuclei” produced via a deep-spallation process of emission of several nucleons during INC, followed by emission of several preequilibrium particles, followed by evaporation of particles and light fragments from compound nuclei, or from fission fragments, if the compound nuclei did fission, as occur in most cases of actinide-induced reactions.

To make the situation even worse, while simulating with high statistics the reaction $^{238}\text{U} + ^{208}\text{Pb}$ shown in Fig. 9, we found several cases where we got *NAN (Not A Number)* results for the angles and velocities of several light fragments. A detailed study showed that we got those bad cases because of using non-relativistic kinematics in GEM2 for transformations from the rest frame of evaporating/fissioning nuclei to the laboratory system (although the kinematics error mentioned above was already fixed). GEM2 as developed by Furihata [7] uses non-relativistic kinematics for such transformations, which is a good enough approximation for CEM, where we calculate only particle-induced reactions, and the velocity of the compound nucleus relative to the Lab system is small. In the case of high-energy heavy-ion reactions, this approximations is not good any more, and in some rare cases can even provide *NAN* results or crash the code. This is why in the FY2009 version of LAQGSM03.03, we replaced the non-relativistic kinematics of GEM2 with a relativistic version, and made also a few small corrections in **subroutine fisgem**, **subroutine stdcay**, and **subroutine rastar**, (in the file **FROMCEM09.f**) for the calculation of the total mass of nuclei, including the excitation energy of the nuclei, to conserve total energy after the transformations. Results from this latest upgrade of LAQGSM03.03 are shown in Figs. 6–9 with green lines and are labeled as “LAQGSM03.03, 2009”. For heavy-ion induced reactions, we see a significant improvement of the results for the mean angles of products $\langle \Theta \rangle$ (see Figs. 7–9) by the “2009” version, and also some improvement of results for the the mean kinetic energy $\langle T(A) \rangle$, while the results for proton-induced reactions (Fig. 6) practically do not change, as expected.

4.C. We corrected an error in **subroutine spectr** of the stand alone LAQGSM03.03 to have the correct output for the K^+ -spectra: This subroutine was modified several times and in a previous version, the array index $JS = 9$ was assigned to ^6Li , providing in the output spectra of ^6Li . The latest version of **spectr** uses this index to identify spectra of K^+ , with “ K^+ ” in the title of the table with spectra, but the index was not corrected in all the right places, until now.

4.D. Gregg Mckinney had a crash while calculating the interaction of 100 GeV/nucleon ^{56}Fe with ^{27}Al with the stand-alone LAQGSM03.01 for a NASA application and asked our help. After a

long investigation, Gudima found that the crash was caused by two small errors in **subroutine dddyk** which calculates $\Delta + \Delta \rightarrow Y + \Delta + K$ channels in the Quark Gluon String Model of LAQGSM, and has fixed it. These channels are very rare and occur with a very low probability only at very high energies, this is why this bug had not crashed LAQGSM previously and the error had not affected the numerous and various reactions we had previously calculated with LAQGSM.

4.E. Nikolai Mokhov encountered an infinite loop in **subroutine cascaw** calculating with LAQGSM interactions of low energy t and ^3He with p in MARS15, and found also several cases of non-conservation of the energy and/or charge, and baryon number for some rare channels of $p + p$ and $d + p$ interactions. Gudima has fixed these problems modifying slightly **subroutine cascaw** and **subroutine typnew** and adding the new subroutines **bbkak**, **pibkak**, **etan**, **pnet**, and **pinkak**.

We have validated the upgraded LAQGSM03.03 against a large number of different reactions induced by ^{56}Fe , ^{48}Ti , ^{40}Ar , ^{35}Cl , ^{28}Si , ^{24}Mg , ^{20}Ne , ^{16}O , ^{14}N , ^{12}C , ^{11}B , ^{10}B , and ^4He of energies from 290 MeV/nucleon to 10 GeV/nucleon on target-nuclei of H, Be, C, Al, Cu, Fe, Sn, and Pb measured recently by the **NASA Measurement Consortium** by Zeitlin et al. (see [17] and references therein). Such measurements are needed for NASA to plan long-duration spaceflights and to test the models used to evaluate radiation exposure in flight, and were performed at many incident energies in this energy range at the Heavy Ion Medical Accelerator in Chiba (HIMAC) and at Brookhaven National Laboratory (see details in [17] and references therein). Such data are also of great interest to test models employed in cancer therapy with carbon ions used currently at several facilities in Europe and Japan and planned to be used in several future cancer treatment centers now under construction.

This is why the authors of these rich measurements have analyzed their data with the widely used one-dimensional semi-phenomenological NASA transport code NUCFRG2 [18], with the microscopic abrasion-ablation model QMSFRG [19], with a parametrization by Nilsen et al. [20], with the well known phenomenological systematics EPAX2 [24], as well as with the recent Japanese transport code PHITS [25].

Examples of LAQGSM03.03 results for 153 reactions induced by projectiles from ^{56}Fe to ^{16}O are compared with experimental data and calculations by several other models in Figs. 10–30. From these results and many other comparisons for other reactions we do not include here, we can conclude that LAQGSM03.03 describes well all these various reactions and provides a better overall agreement with the data as compared with the NASA code NUCFRG2 [18], the abrasion-ablation model QMSFRG [19], and the parametrization by Nilsen et al. [20]. In Ref. [22], we have shown that LAQGSM03.03 describes quite well also reactions induced by ^{12}C , and agrees with the measured data better than EPAX2 [24], NUCFRG2 [18], and PHITS [25] do, especially if we look at the He production cross sections (see Figs. 6 and 7 of Ref. [22]).

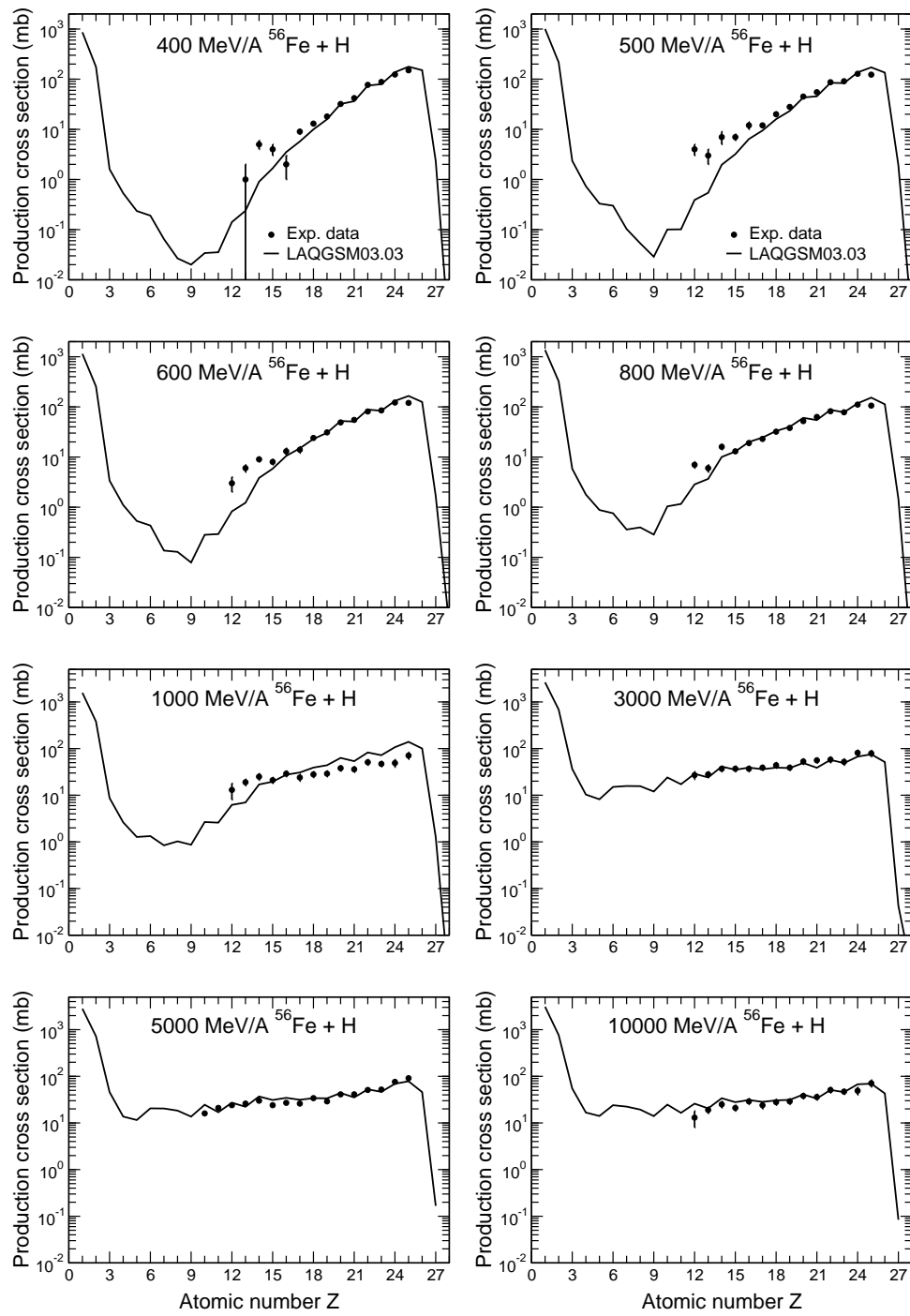


Figure 10: Atomic-number dependence of the fragment-production cross sections from the interactions of ^{56}Fe of about 400, 500, 600, 800, 1000, 3000, 5000, and 10000 MeV/nucleon with H. Experimental data (circles) are by Zeitlin et al. [17], while lines show results by LAQGSM03.03.

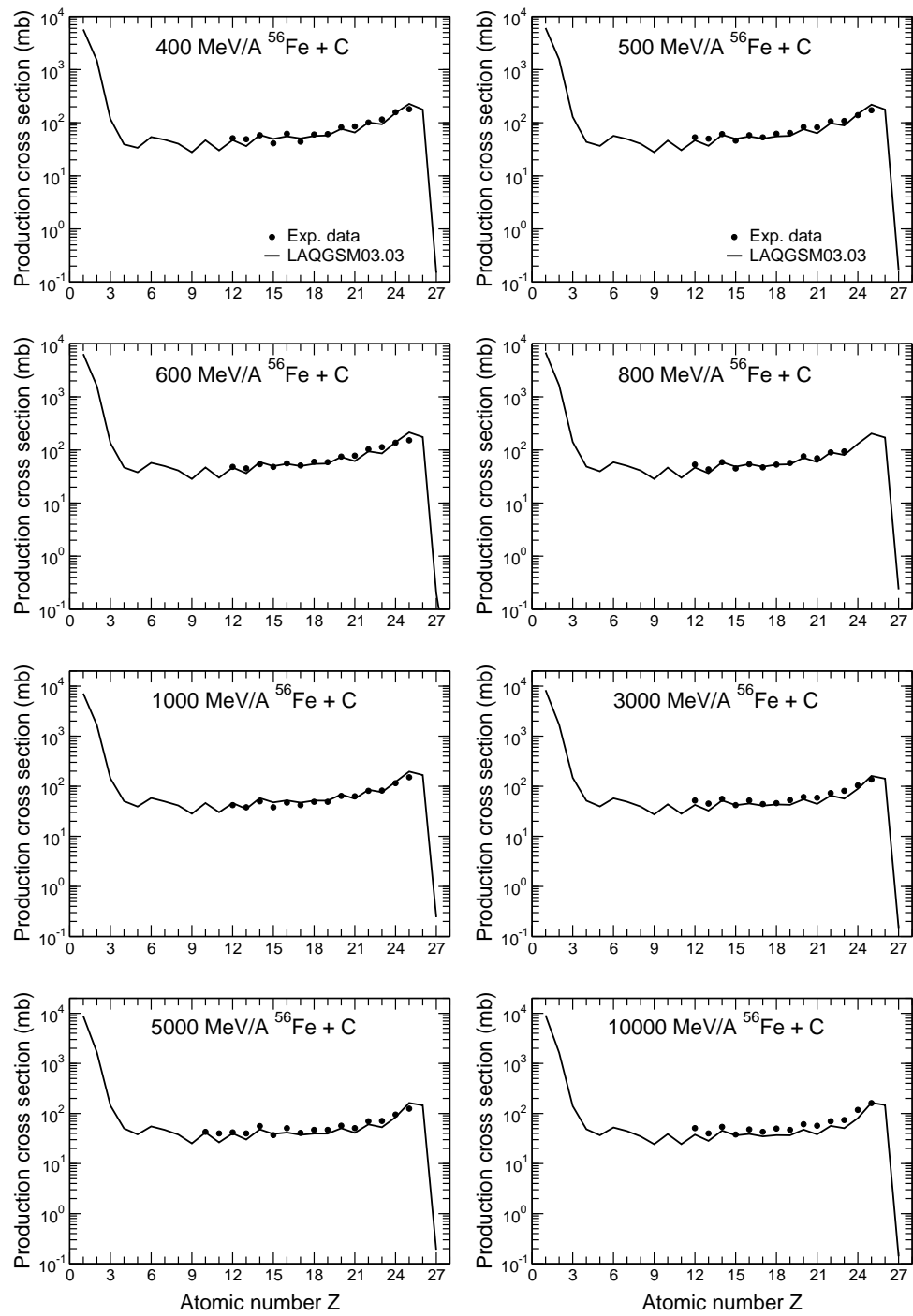


Figure 11: The same as in Fig. 10 but for interactions with C.

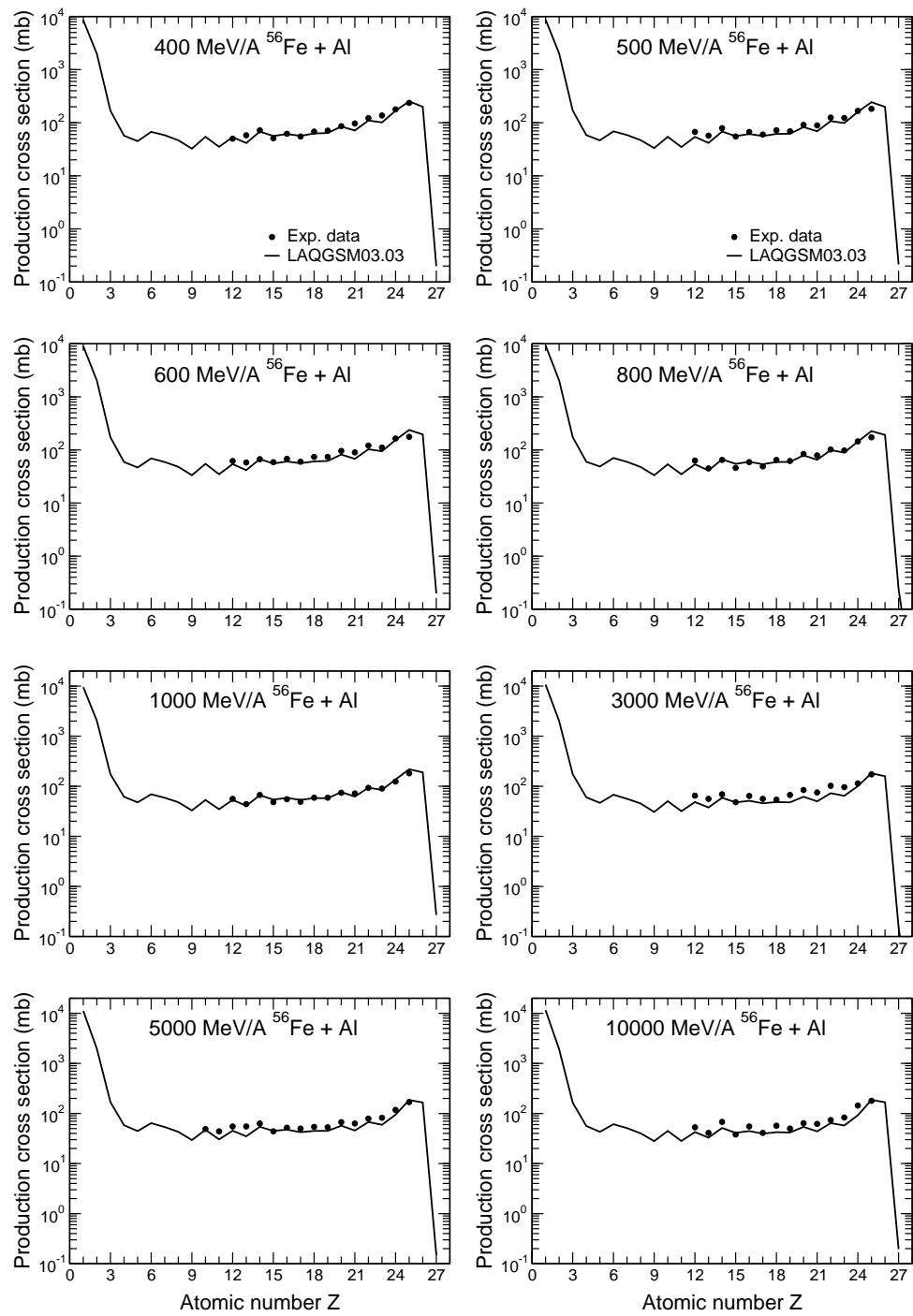


Figure 12: The same as in Fig. 10 but for interactions with Al.

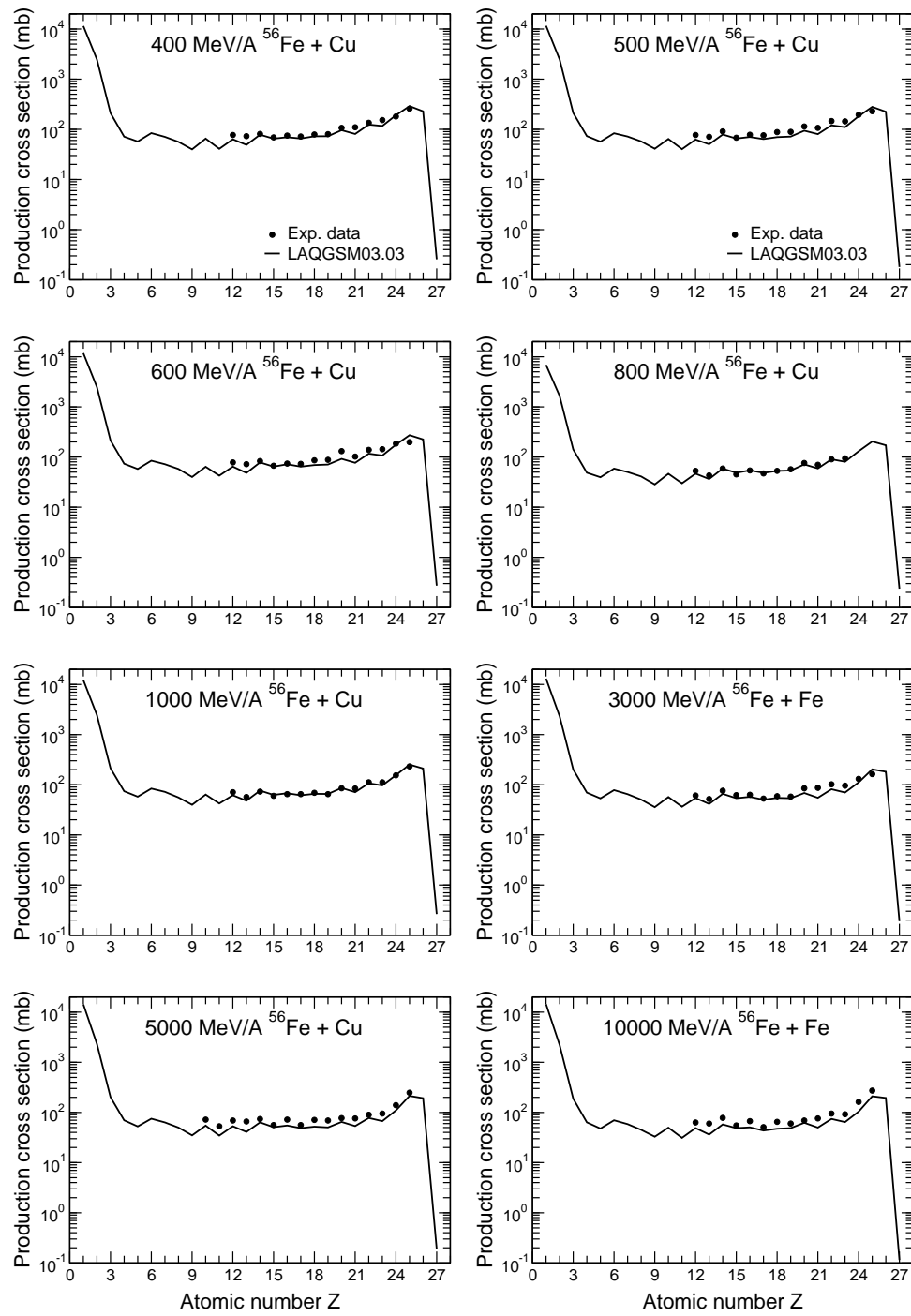


Figure 13: The same as in Fig. 10 but for interactions with Cu(Fe).

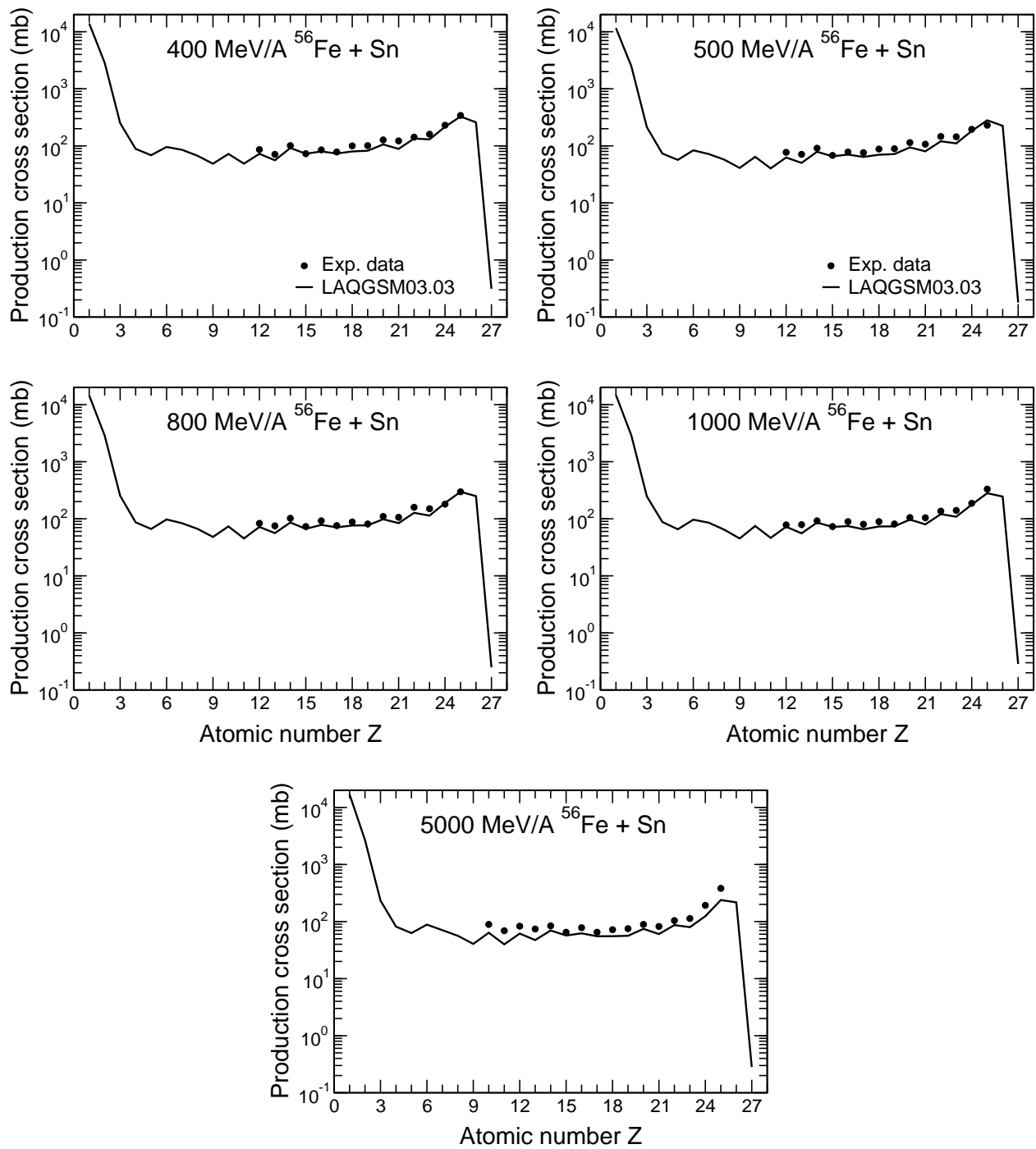


Figure 14: The same as in Fig. 10 but for interactions with Sn at 400, 500, 800, 1000, and 5000 MeV/nucleon.

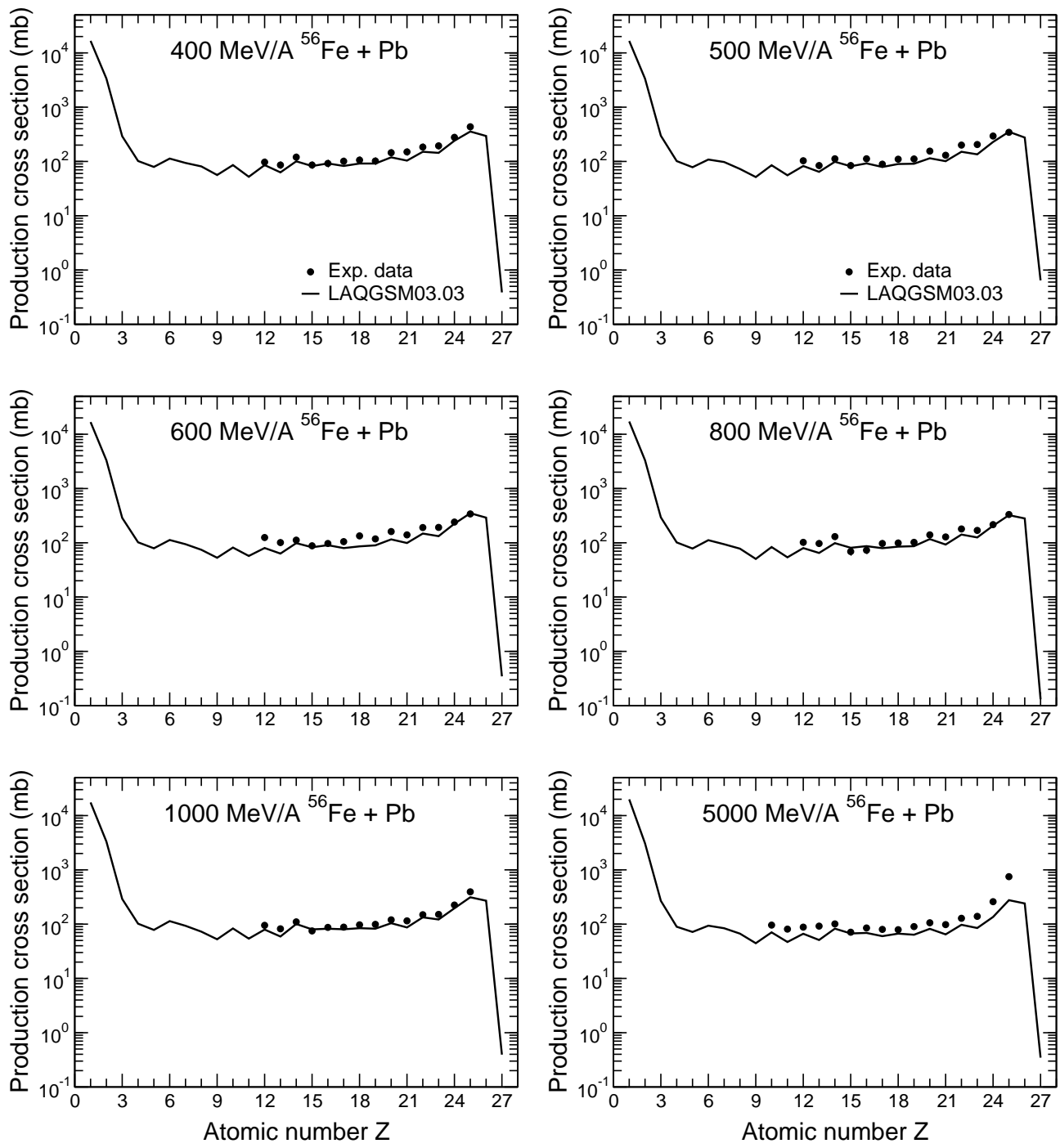


Figure 15: The same as in Fig. 10 but for interactions with Pb at 400, 500, 600, 800, 1000, and 5000 MeV/nucleon.

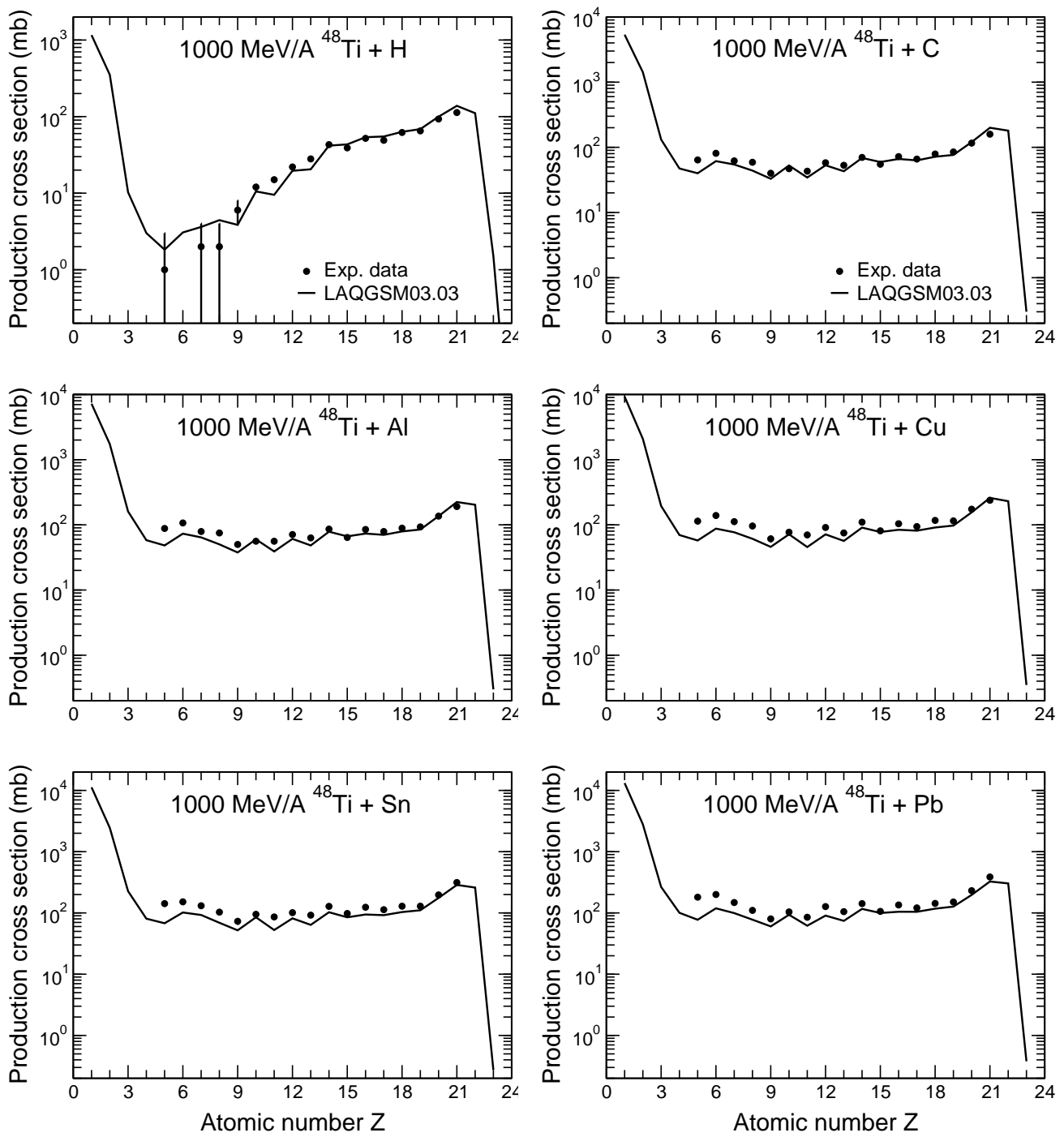


Figure 16: The same as in Fig. 10 but for interaction of ^{48}Ti with H, C, Al, Cu, Sn, and Pb at 1 GeV/nucleon.

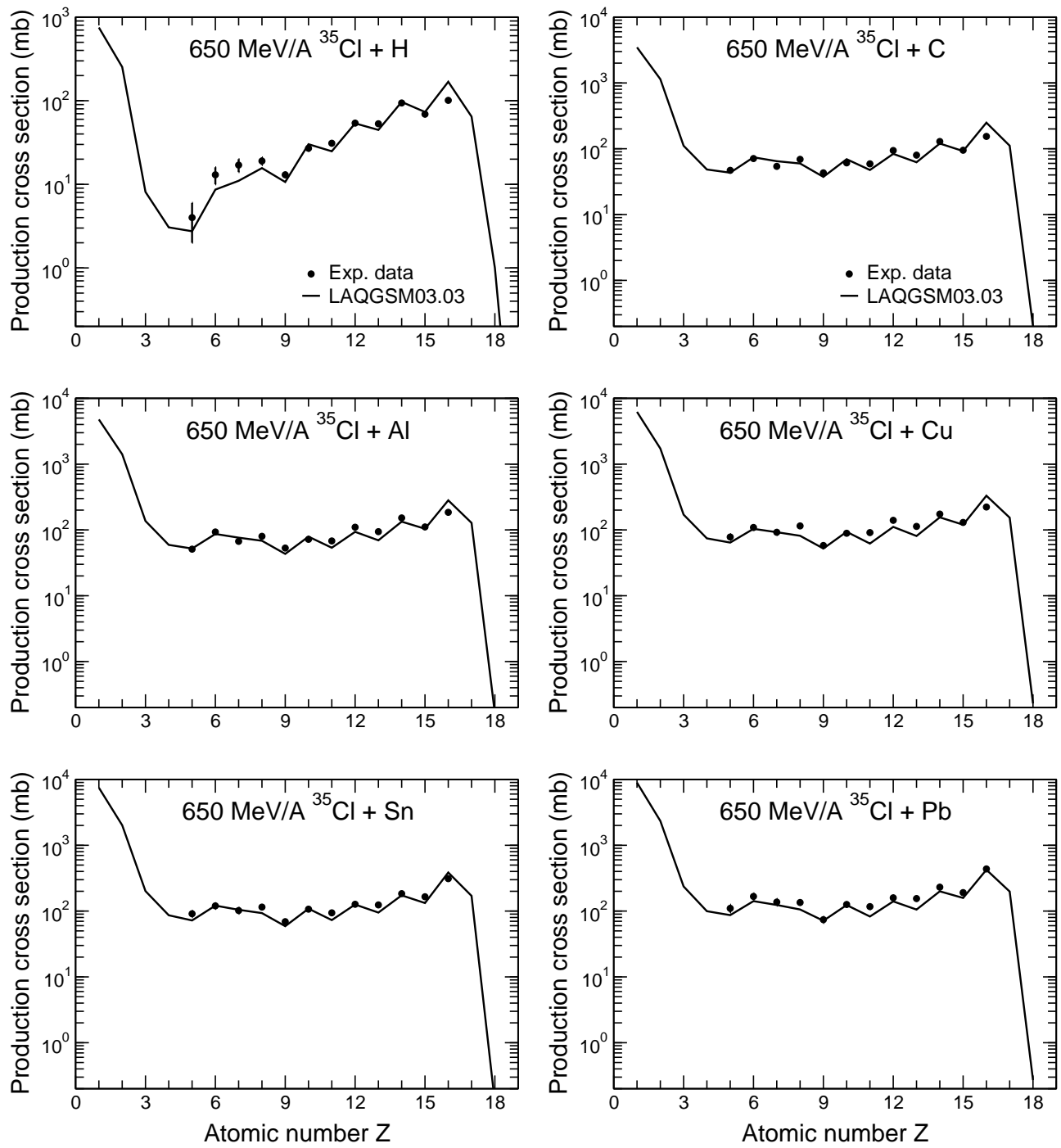


Figure 17: The same as in Fig. 10 but for interaction of ^{35}Cl with H, C, Al, Cu, Sn, and Pb at 650 MeV/nucleon.

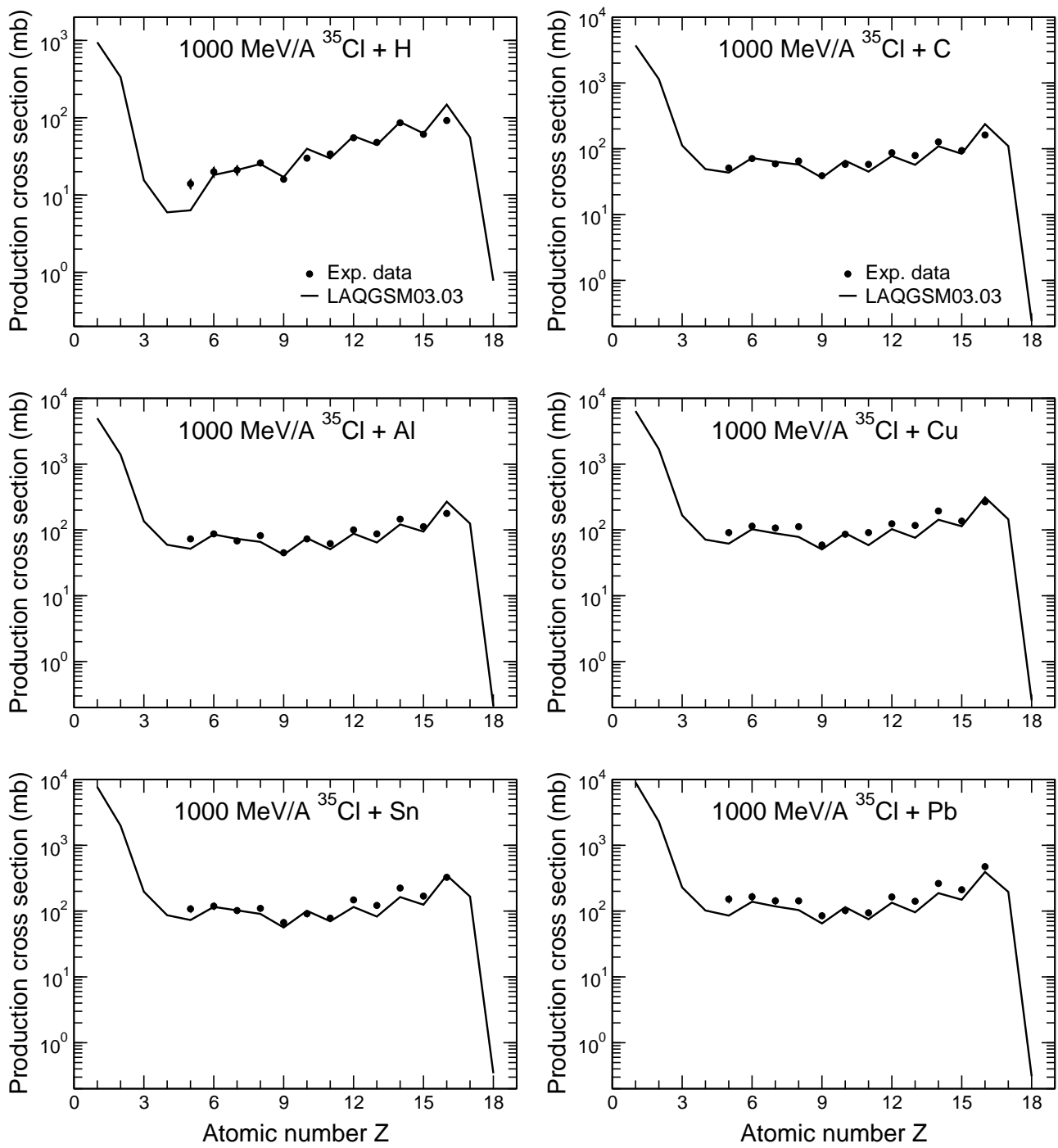


Figure 18: The same as in Fig. 10 but for interaction of ^{35}Cl with H, C, Al, Cu, Sn, and Pb at 1 GeV/nucleon.

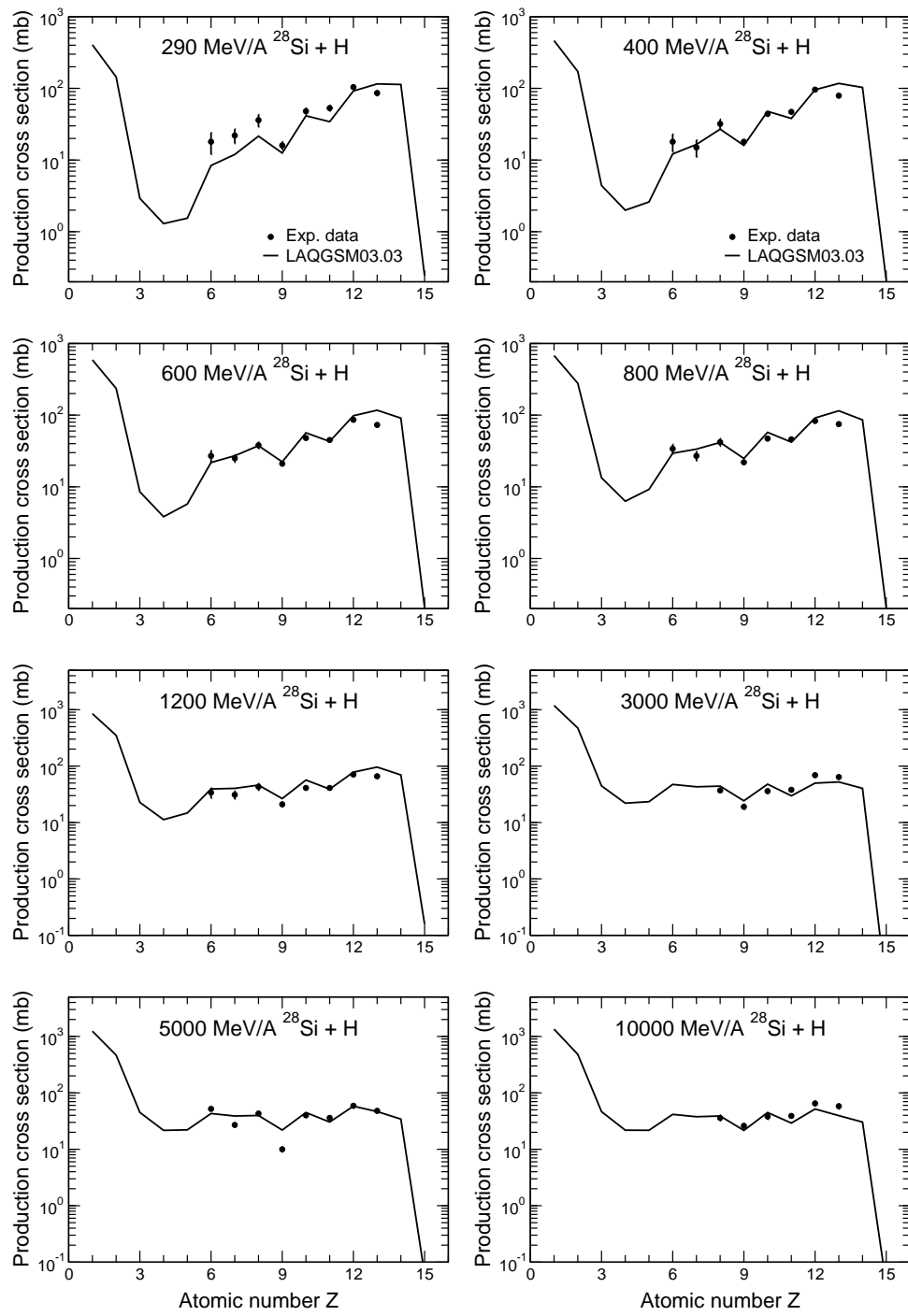


Figure 19: The same as in Fig. 10 but for interactions of ^{28}Si at 290, 400, 600, 800, 1200, 3000, 5000, and 10000 MeV/nucleon with H.

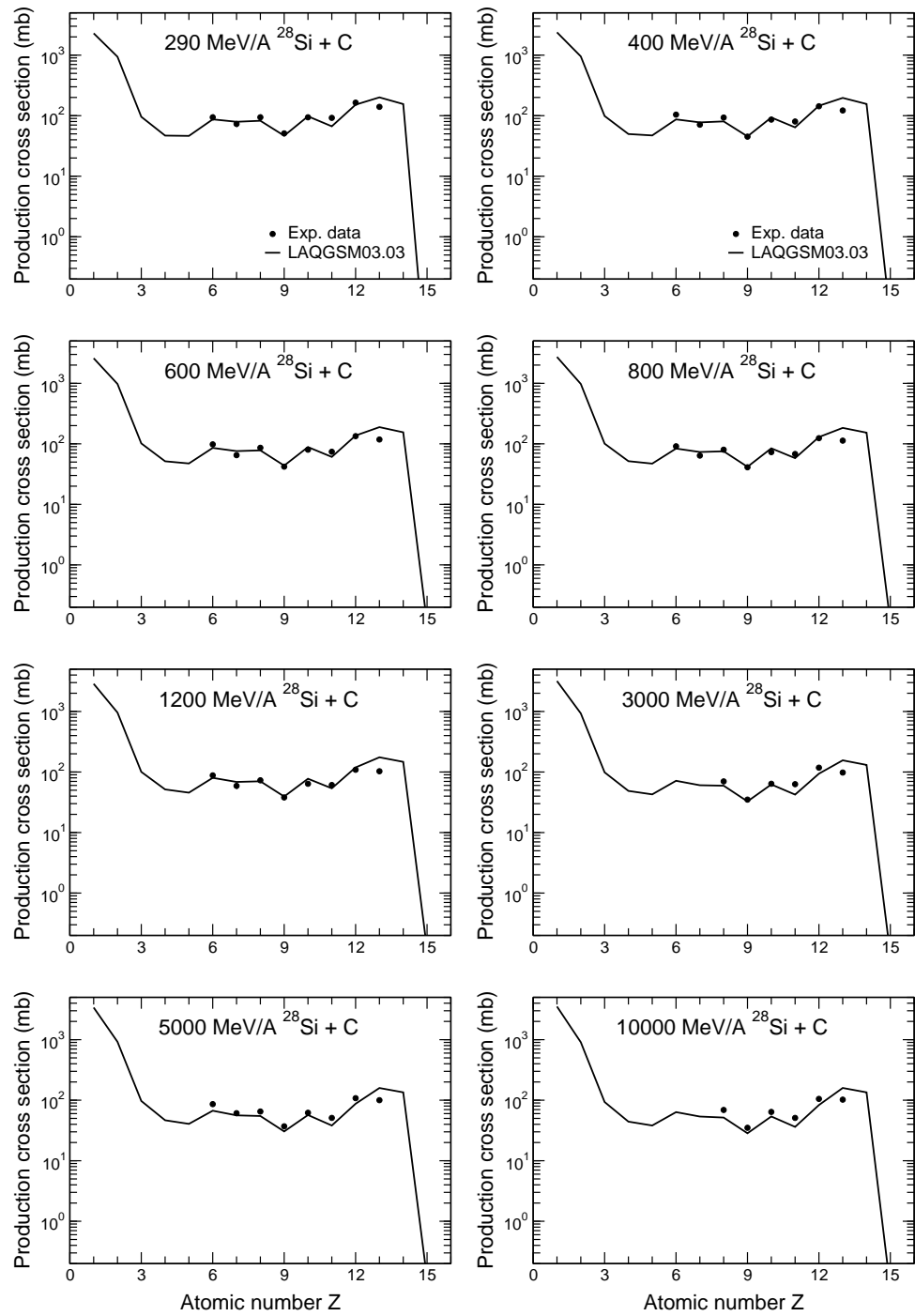


Figure 20: The same as in Fig. 19 but for interactions with C.

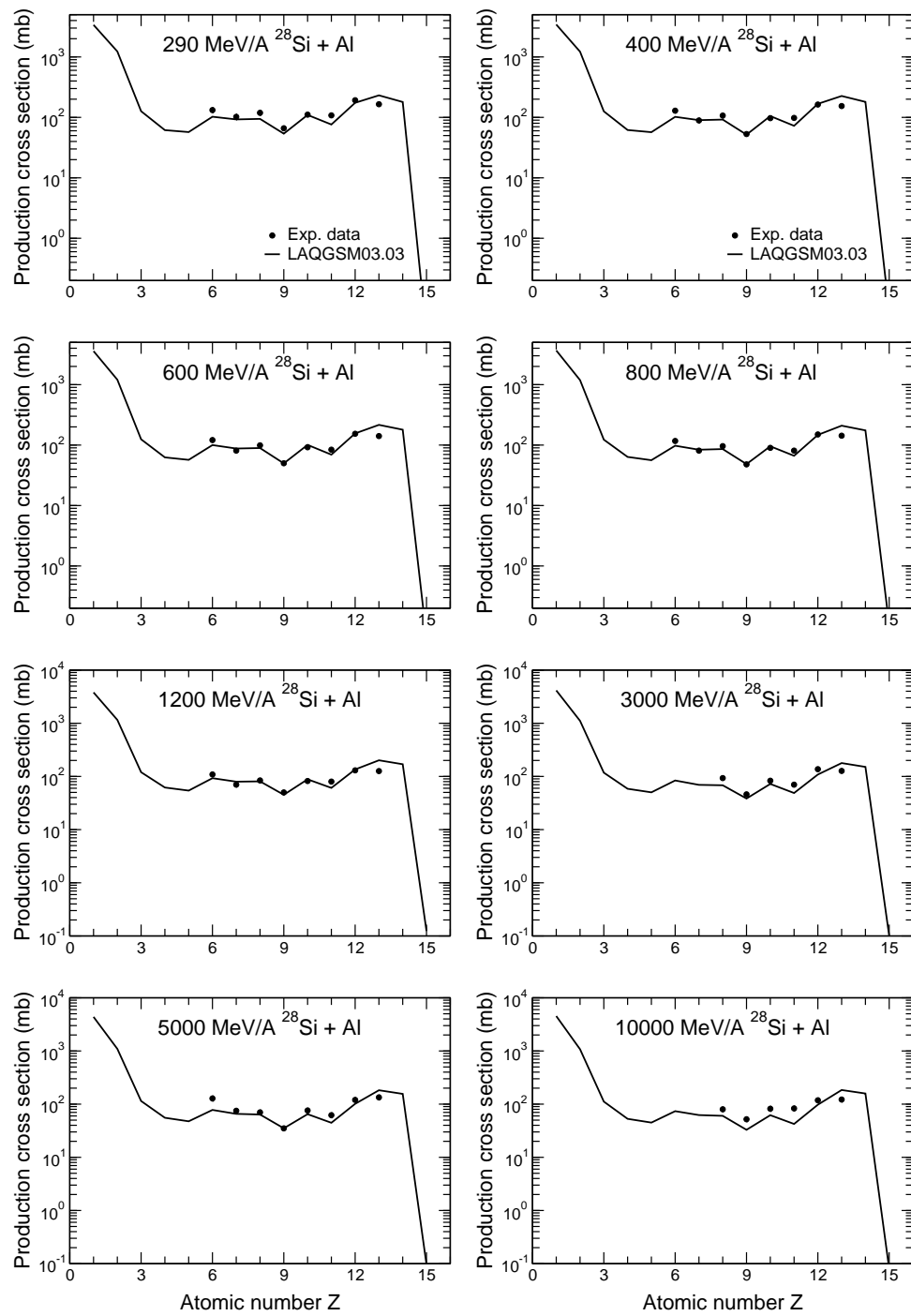


Figure 21: The same as in Fig. 19 but for interactions with Al.

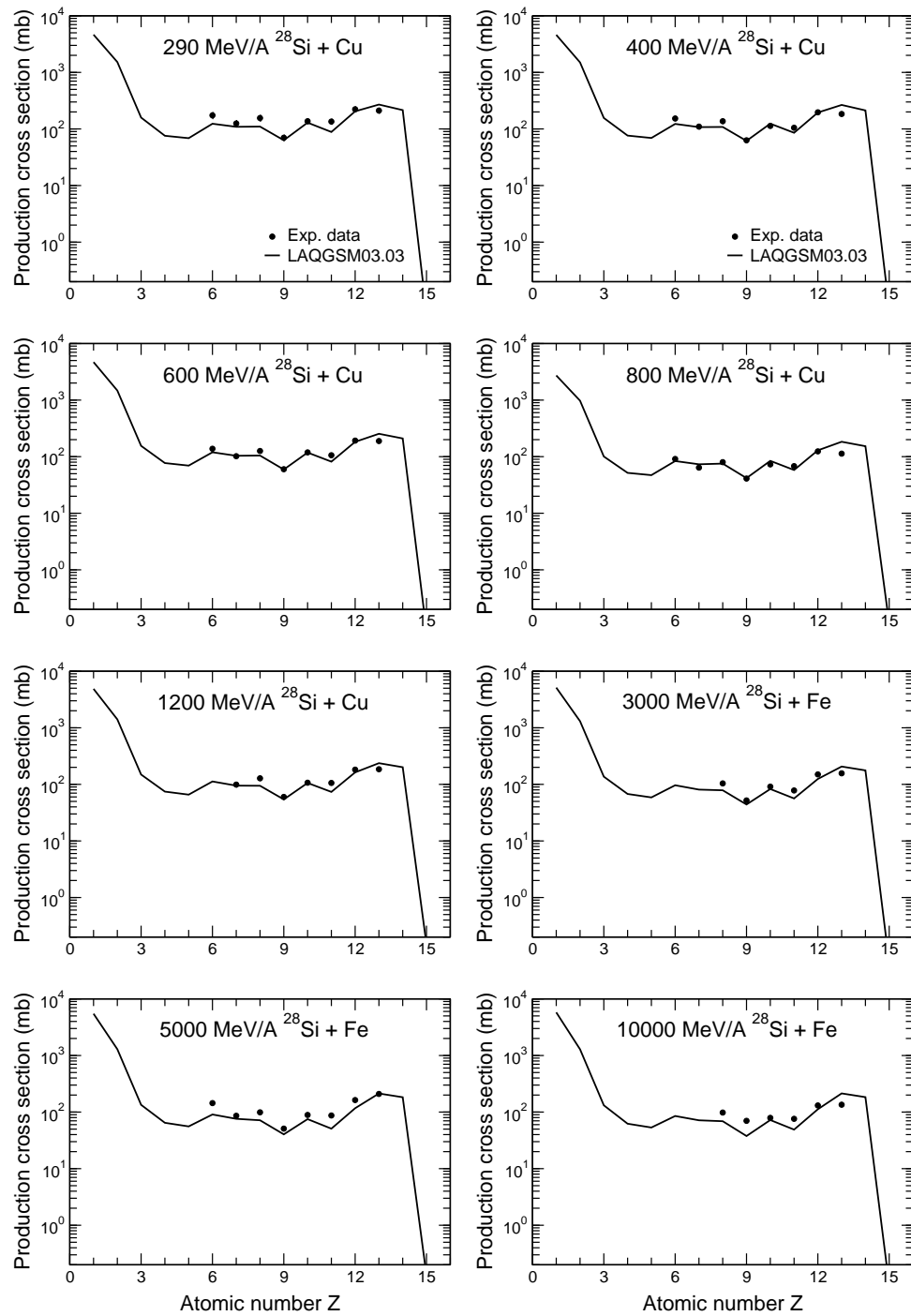


Figure 22: The same as in Fig. 19 but for interactions with Cu(Fe).

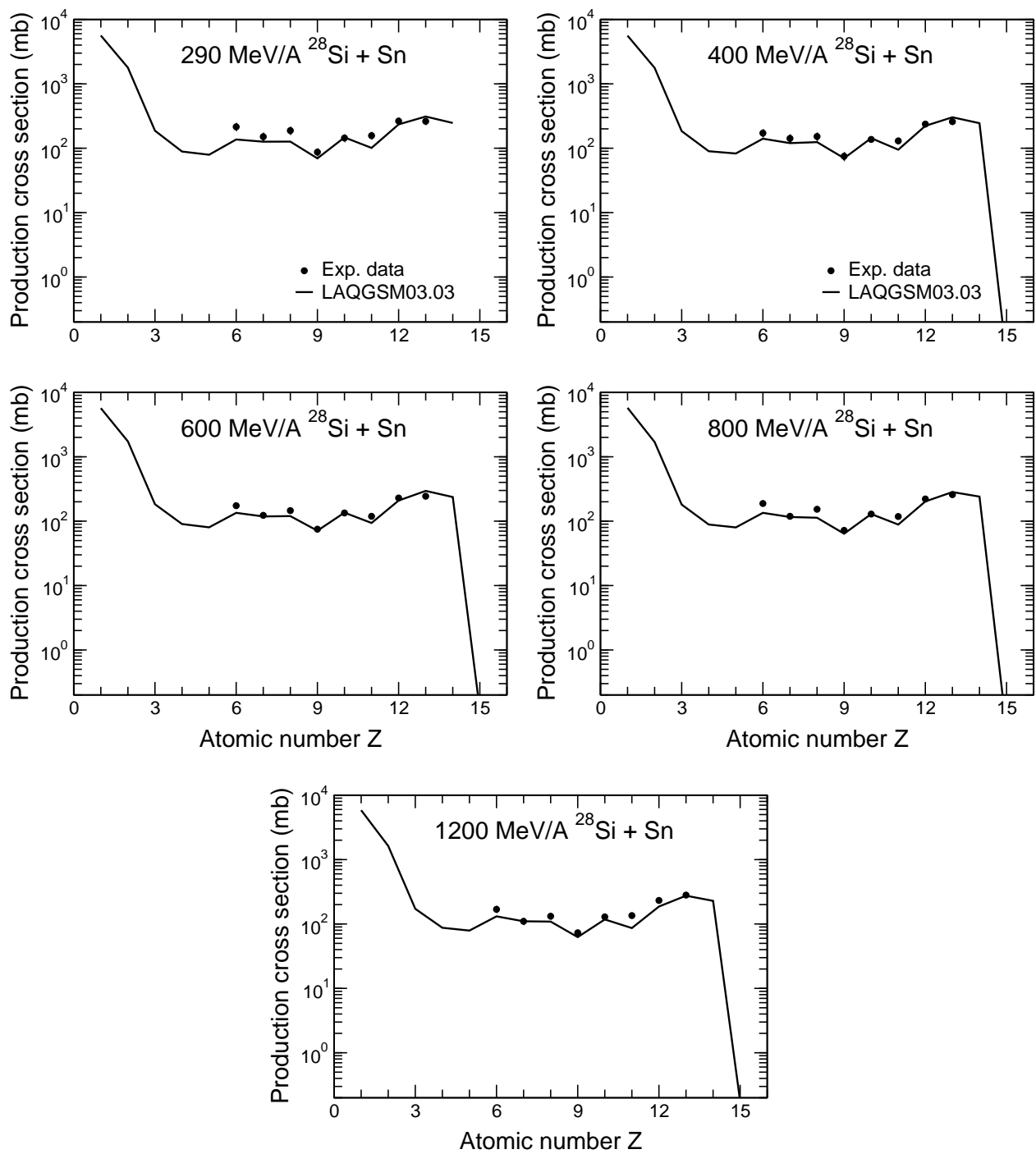


Figure 23: The same as in Fig. 19 but for interactions with Sn at 290, 400, 600, 800, and 1200 MeV/nucleon.

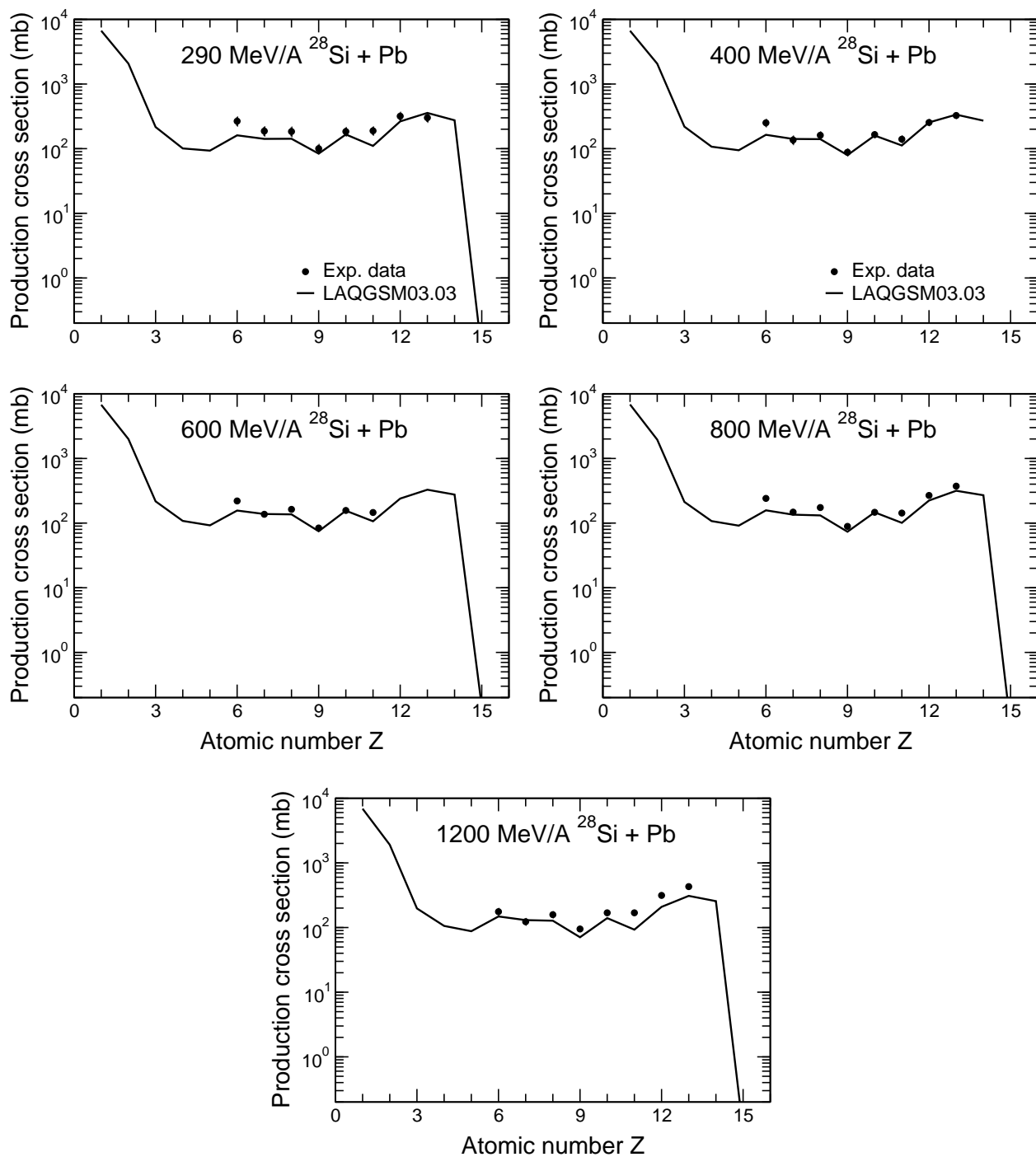


Figure 24: The same as in Fig. 23 but for interactions with Pb.

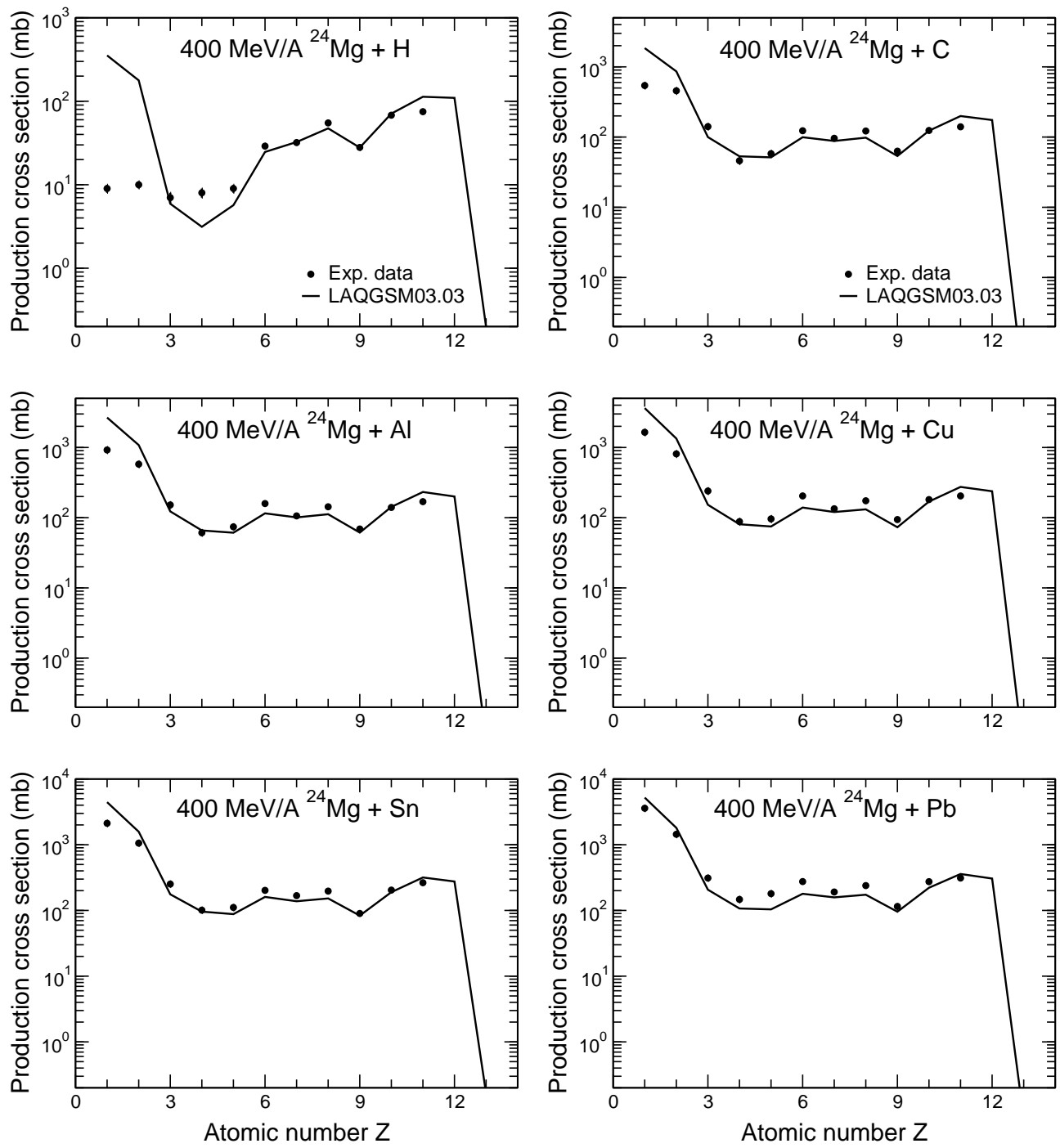


Figure 25: The same as in Fig. 10 but for interactions of ${}^{24}\text{Mg}$ at 400 MeV/nucleon with H, C, Al, Cu, Sn, and Pb.

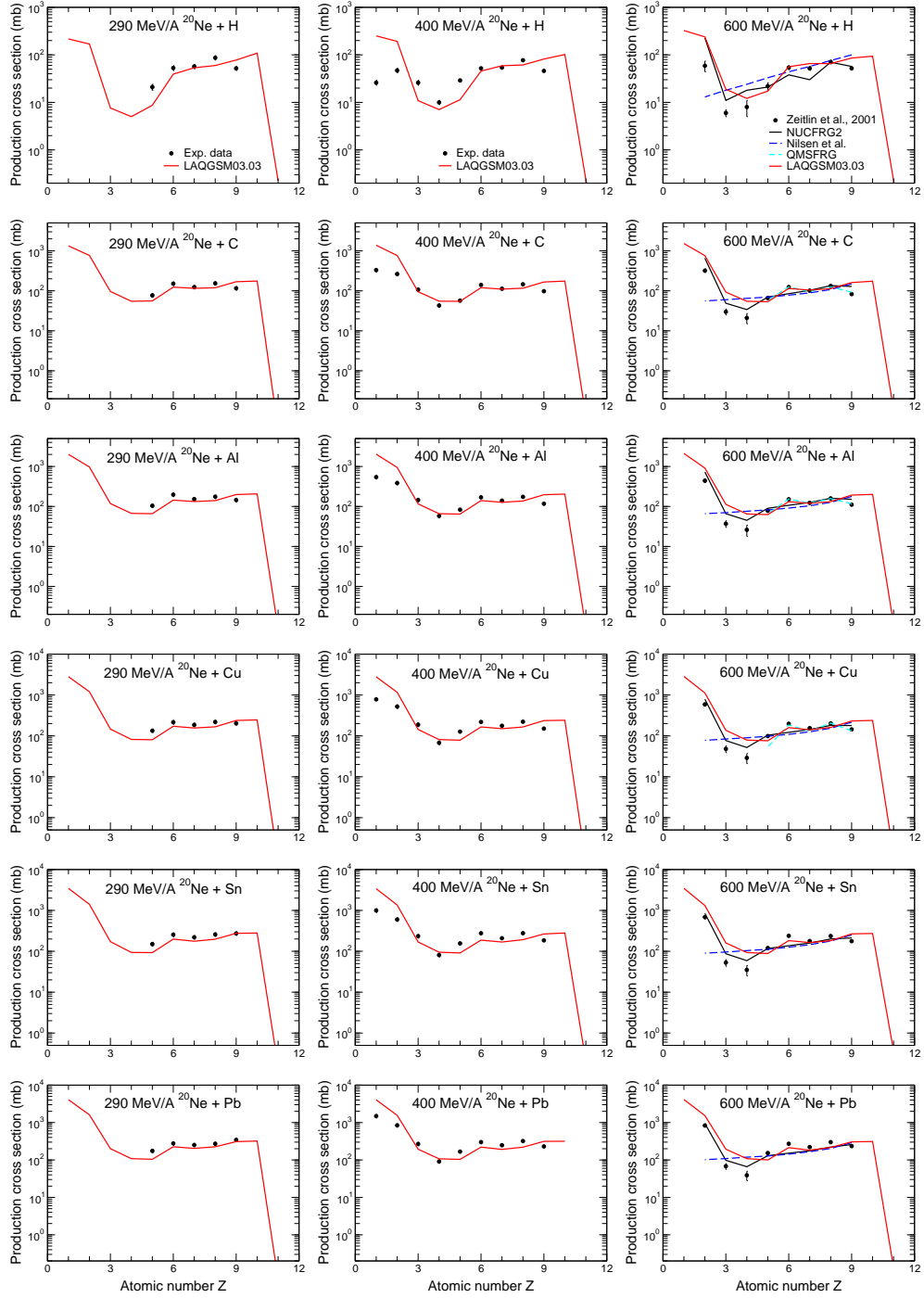


Figure 26: The same as in Fig. 10 but for interactions of 290, 400, and 600 MeV/nucleon ^{20}Ne with H, C, Al, Cu, Sn, and Pb. For comparison, at 600 MeV/A, results by the NASA semi-empirical nuclear fragmentation code NUCFRG2 [18] and the microscopic abrasion-ablation model QMSFRG [19], as well as from a parametrization by Nilsen et al. [20] taken from Tab. III of Ref. [21] are shown with different colors, as indicated.

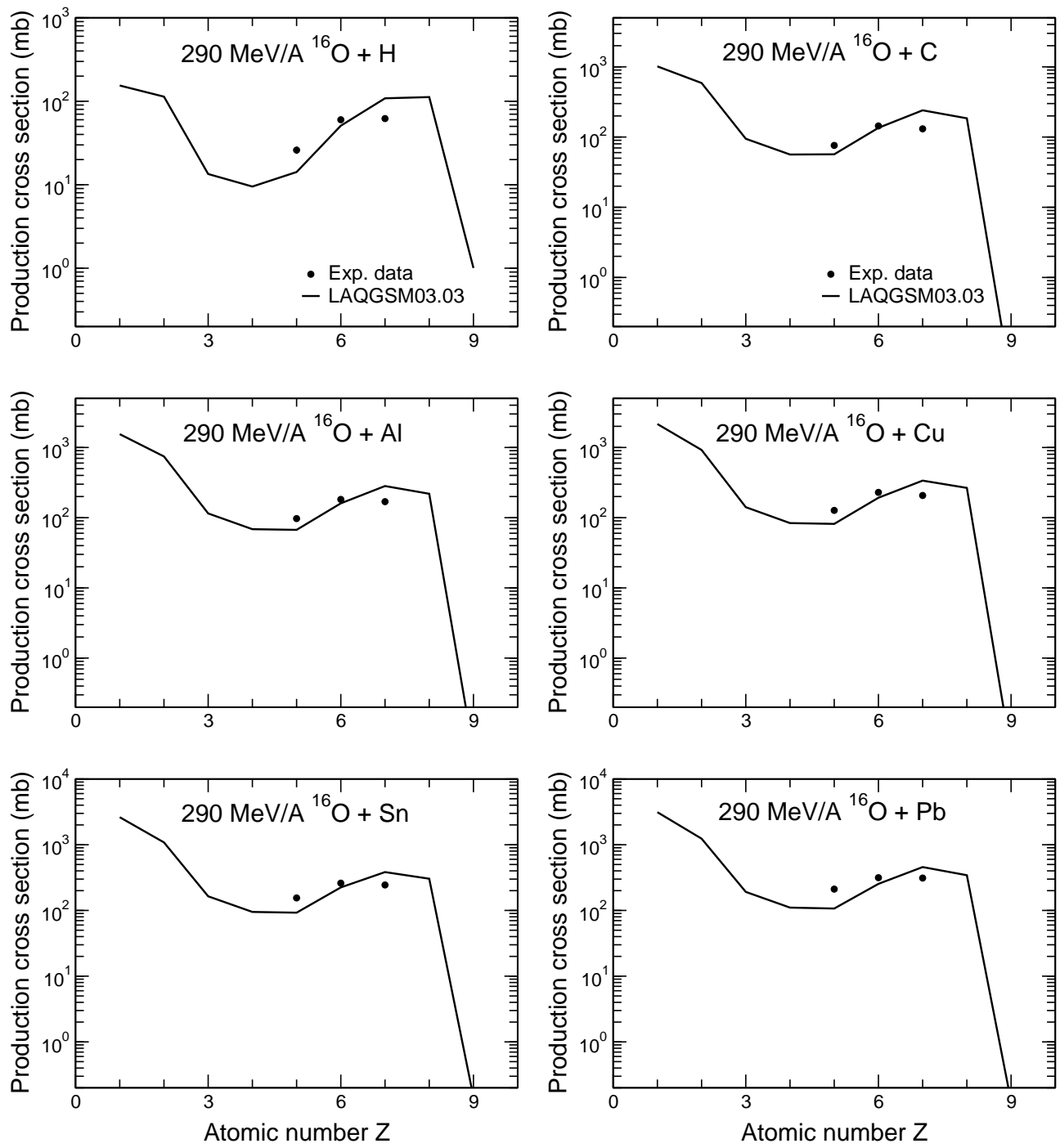


Figure 27: The same as in Fig. 10 but for interactions of ^{16}O at 290 MeV/nucleon with H, C, Al, Cu, Sn, and Pb.

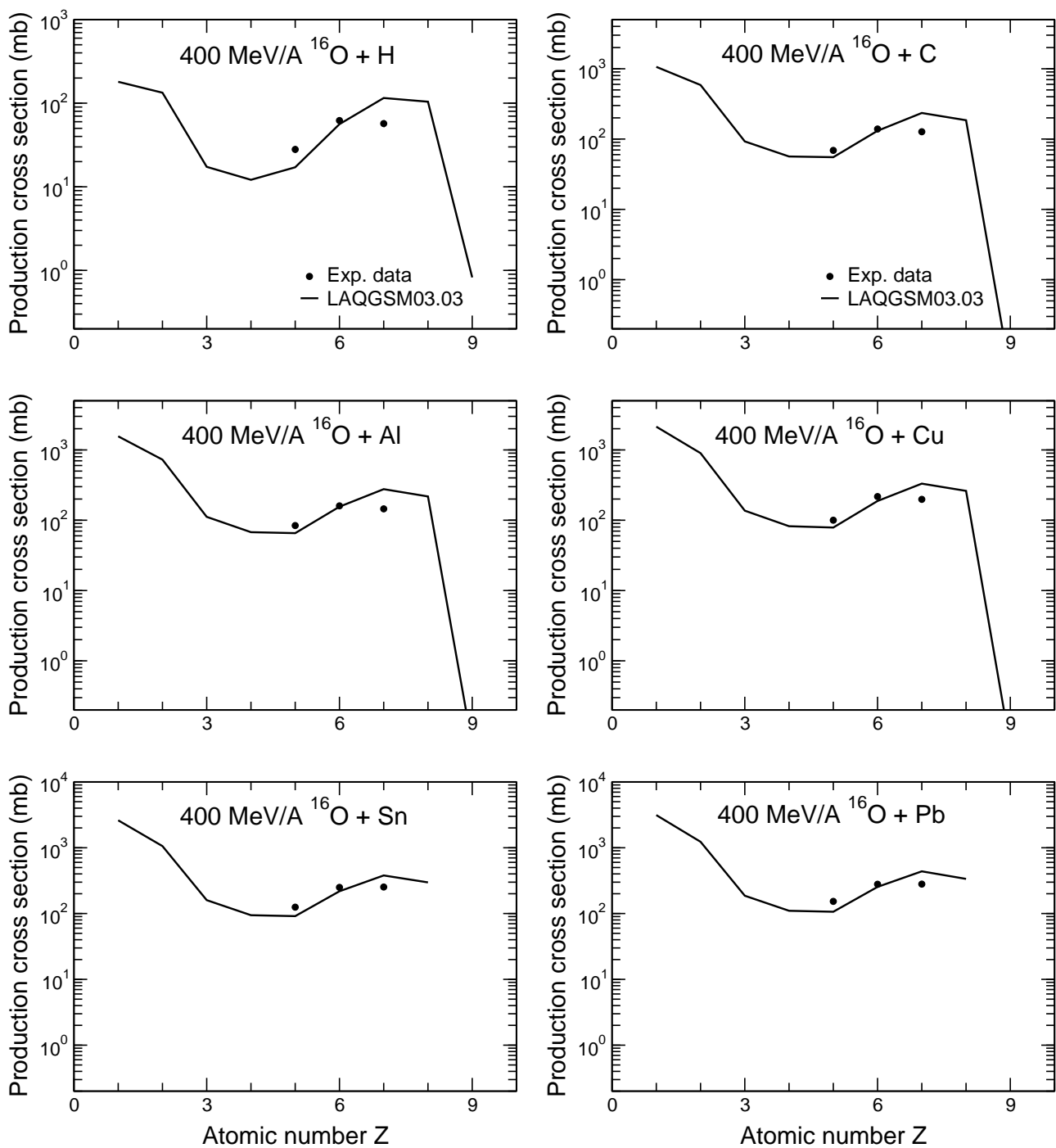


Figure 28: The same as in Fig. 27 but for interactions at 400 MeV/nucleon.

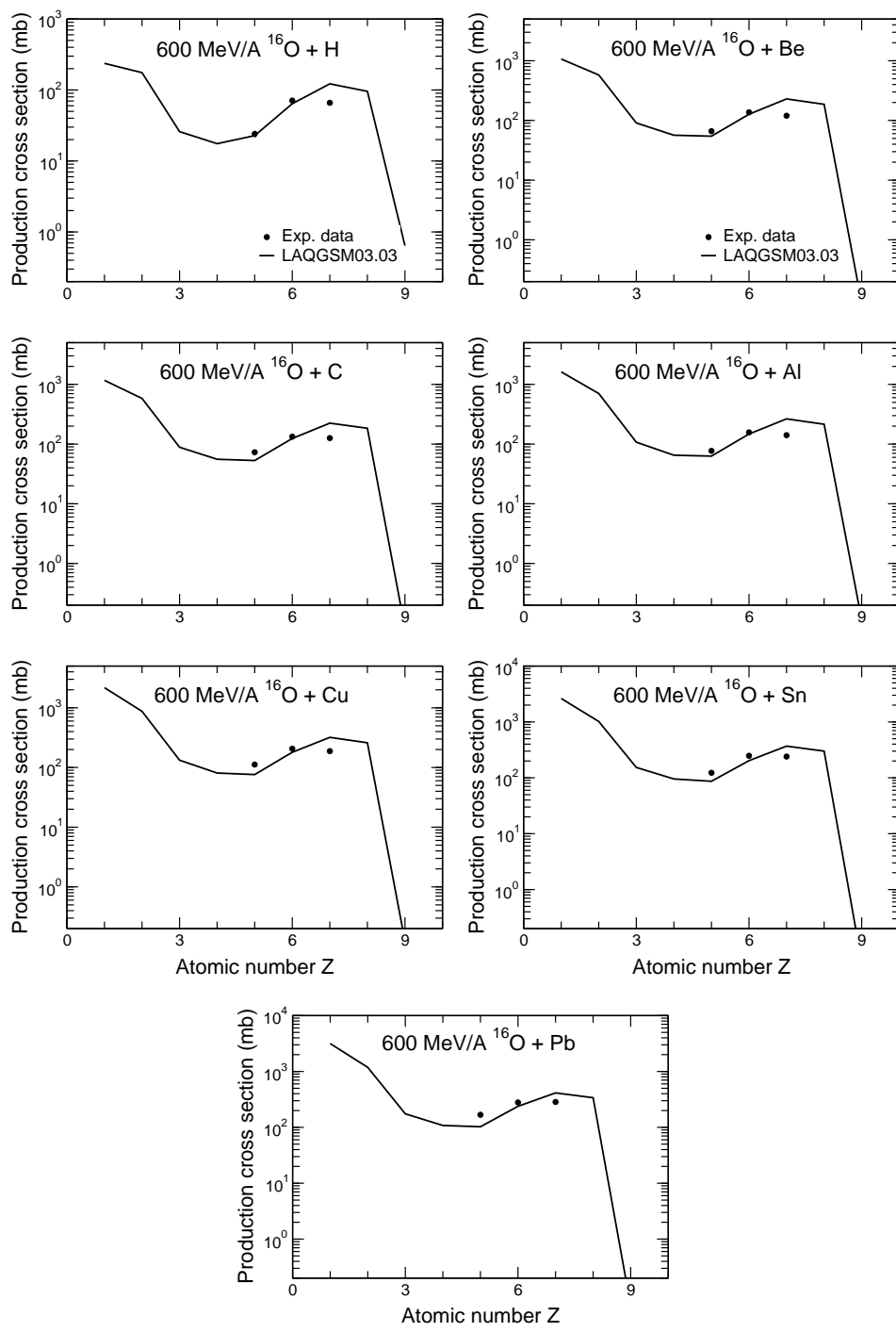


Figure 29: The same as in Fig. 10 but for interactions of ^{16}O at 600 MeV/nucleon with H, Be, C, Al, Cu, Sn, and Pb.

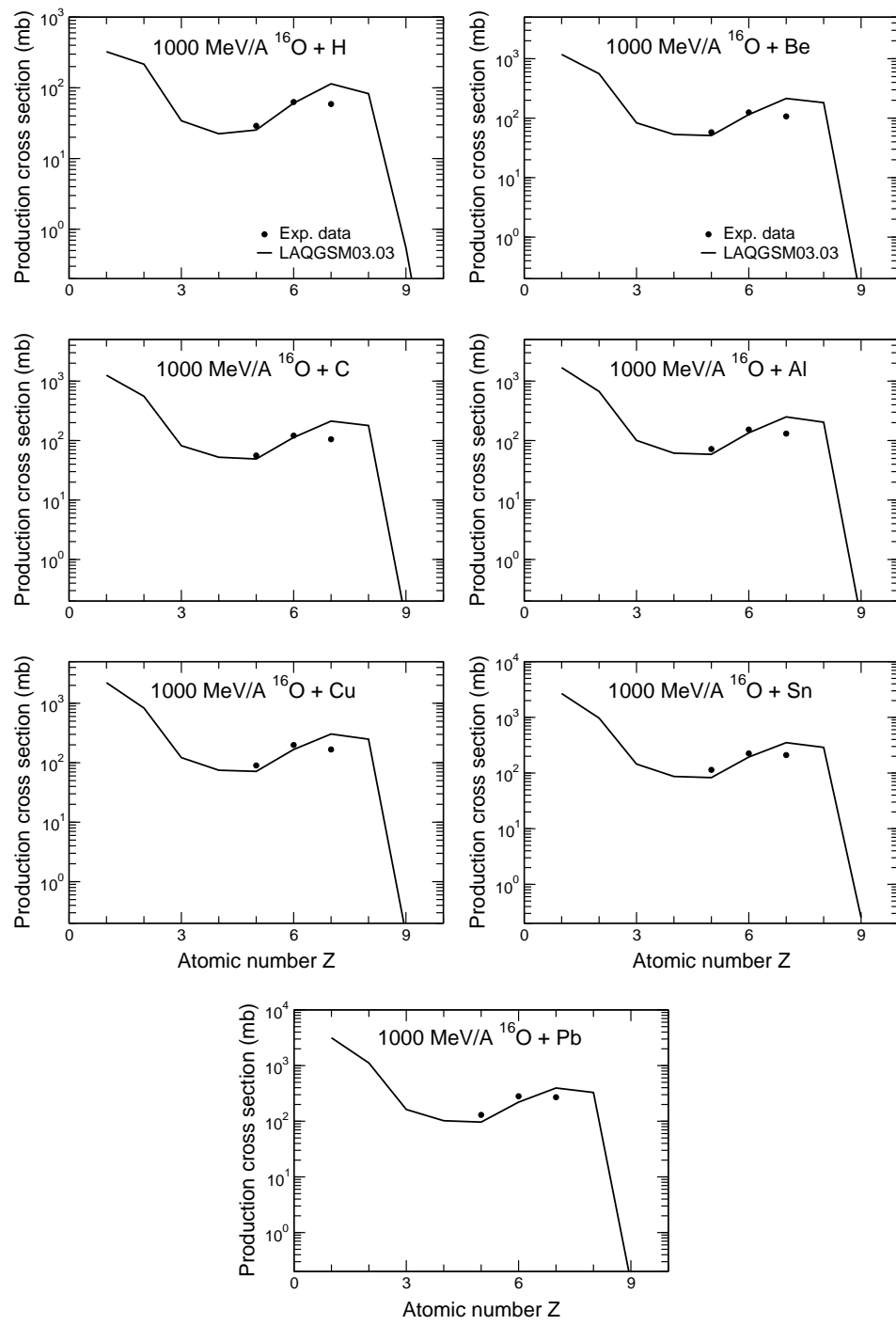


Figure 30: The same as in Fig. 29 but for interactions at 1 GeV/nucleon.

Acknowledgment

This work was carried out under the auspices of the U. S. Department of Energy (DOE).

REFERENCES

- [1] S. G. Mashnik, M. I. Baznat, K. K. Gudima, A. J. Sierk, and R. E. Prael, “CEM03 and LAQGSM03: Extension of the CEM2k+GEM2 and LAQGSM Codes to Describe Photo-Nuclear Reactions at Intermediate Energies (30 MeV to 1.5 GeV),” *J. Nucl. Radiochem. Sci.* **6** (2005) A1–A19; (E-print: nucl-th/0503061).
- [2] S. G. Mashnik, K. K. Gudima, A. J. Sierk, M. I. Baznat, and N. V. Mokhov, *CEM03.01 User Manual*, LANL Report LA-UR-05-7321, Los Alamos, 2005; RSICC Code Package PSR-532, <http://www-rsicc.ornl.gov/codes/psr/psr5/psr-532.html>.
- [3] K. K. Gudima, S. G. Mashnik, and V. D. Toneev, “Cascade-Exciton Model of Nuclear Reactions,” *Nucl. Phys.* **A401** (1983) 329–361.
- [4] K. K. Gudima, S. G. Mashnik, and A. J. Sierk, *User Manual for the Code LAQGSM*, LANL Report LA-UR-01-6804, Los Alamos, 2001.
- [5] K. K. Gudima and S. G. Mashnik, “Extension of the LAQGSM03 Code to Describe Photo-Nuclear Reactions up to Tens of GeV,” Proc. 11th Int. Conf. on Nuclear Reaction Mechanisms, Varenna, Italy, June 12–16, 2006, edited by E. Gadioli, Ricerca Scientifica ed Educazione Permanente, Supplemento N. 126, 2006, pp. 525–534; (E-print: nucl-th/0607007).
- [6] S. G. Mashnik, K. K. Gudima, R. E. Prael, A. J. Sierk, M. I. Baznat, and N. V. Mokhov, “CEM03.03 and LAQGSM03.03 Event Generators for the MCNP6, MCNPX, and MARS15 Transport Codes,” Invited lectures presented at the Joint ICTP-IAEA Advanced Workshop on Model Codes for Spallation Reactions, February 4–8, 2008, ICTP, Trieste, Italy, LA-UR-08-2931, Los Alamos (2008); E-print: arXiv:0805.0751v2 [nucl-th]; IAEA Report INDC(NDS)-0530, Distr. SC, Vienna, Austria, August 2008, p. 51.
- [7] S. Furihata, “Statistical Analysis of Light Fragment Production from Medium Energy Proton-Induced Reactions,” *Nucl. Instr. Meth. B* **171** (2000) 252; *Development of a generalized evaporation model and study of residual nuclei production*, Ph.D. thesis, Tohoku University, Japan, 2003, and references therein.
- [8] F. Rejmund, B. Mustapha, P. Armbruster, J. Benlliure, M. Bernas, A. Boudard, J. P. Dufour, T. Enqvist, R. Legrain, S. Leray, K.-H. Schmidt, C. Stéphan, J. Taieb, L. Tassan-Got, and C. Volant, “Measurement of Isotopic Cross Sections of Spallation Residues in 800 A MeV ^{197}Au + p Collisions,” *Nucl. Phys.* **A683** (2001) 540–565; J. Benlliure, P. Armbruster, M. Bernas, A. Boudard, J. P. Dufour, T. Enqvist, R. Legrain, S. Leray, B.

- Mustapha, F. Rejmund, K.-H. Schmidt, C. Stéphan, L. Tassan-Got, and C. Volant, “Isotopic Production Cross Sections of Fission Residues in ^{197}Au -on-Proton Collisions at 800 A MeV,” Nucl. Phys. **A683** (2001) 513–539.
- [9] J. Taieb, K.-H. Schmidt, L. Tissan-Got, P. Armstrong, J. Benlliure, M. Bernas, A. Boudard, E. Casarejos, S. Czajkowski, T. Enqvist, R. Legrain, S. Leray, B. Mustapha, M. Pravikoff, F. Rejmund, C. Stéphan, C. Volant, and W. Wlazlo, “Evaporation Residues Produced in the Spallation Reaction $^{238}\text{U} + p$ at 1 A GeV,” Nucl. Phys. **A724** (2003) 413–430; M. Bernas, P. Armstrong, J. Benlliure, A. Boudard, E. Casarejos, S. Czajkowski, T. Enqvist, R. Legrain, S. Leray, B. Mustapha, P. Napolitani, J. Pereira, F. Rejmund, M.-V. Ricciardi, K.-H. Schmidt, C. Stéphan, J. Taieb, L. Tissan-Got, and C. Volant, “Fission-Residues Produced in the Spallation Reaction $^{238}\text{U} + p$ at 1 A GeV,” Nucl. Phys. **A725** (2003) 213–253.
- [10] *Benchmark of Spallation Models*,
http://nds121.iaea.org/alberto/mediawiki-1.6.10/index.php/Main_Page.
- [11] K. K. Gudima, M. I. Baznat, S. G. Mashnik, and A. J. Sierk, “Benchmarking the CEM03.03 Event Generator,” LANL Report LA-UR-09-03047, Los Alamos (2009), presentation (view-graphs) at the International Topical Meeting on Nuclear Research Applications and Utilization of Accelerators (AccApp’09), 4–8 May 2009, IAEA, Vienna, Austria,
<http://nds121.iaea.org/alberto/mediawiki-1.6.10/images/7/76/LA-UR-09-03047.pdf>.
- [12] M. I. Baznat, K. K. Gudima, S. G. Mashnik, and A. J. Sierk, “Complex particle production by CEM03.03,” LANL Report LA-UR-09-03046, Los Alamos (2009), poster presented at the International Topical Meeting on Nuclear Research Applications and Utilization of Accelerators (AccApp’09), 4–8 May 2009, IAEA, Vienna, Austria,
<http://nds121.iaea.org/alberto/mediawiki-1.6.10/images/6/62/LA-UR-09-03046.pdf>.
- [13] J. Franz, P. Koncz, E. Rössle, C. Sauerwein, H. Schmitt, K. Schmoll, Erö, Z. Fodor, J. Kecskeméti, Zs. Kovács, and Z. Seres, “Neutron-induced production of protons, deuterons and tritons on copper” Nucl. Phys. **A510** (1999) 774–802.
- [14] A. A. Cowley, G. J. Arendse, J. W. Koen, W. A. Richter, J. A. Stander, G. F. Steyn, P. Demetriou, P. E. Hodgson, and Y. Watanabe “Inclusive (p, α) reactions on ^{27}Al , ^{59}Co , and ^{197}Au at incident energies of 120, 160, and 200 MeV,” Phys. Rev. C **54** (1996) 778–783.
- [15] I. Dostrovsky, R. Davis, Jr., A. M. Poskanzer, and P. L. Reeder, “Cross Sections for the Production of Li^9 , C^{16} , and N^{17} in Irradiations with GeV-Energy Protons,” Phys. Rev. **139** (1996) B1513-B1524; I. Dostrovsky, H. Gauvin, and M. Lefort, “ (p, xp) and $(p, xpy\alpha)$ Reactions of 156-MeV Protons with Light Targets ($A = 11$ to $A = 27$),” Phys. Rev. **169** (1996) 836–841.
- [16] T. Enqvist, J. Benlliure, F. Farget, K.-H. Schmidt, P. Armbruster, M. Bernas, L. Tassan-Got, A. Boudard, R. Legrain, C. Volant, C. Boeckstiegel, M. de Jong, and J. P. Dufour, “Systematic Experimental Survey on Projectile Fragmentation and Fission Induced

- in Collisions of ^{238}U at 1 A GeV with Lead," Nucl. Phys. **A658** (1999) 47–66.
- [17] C. Zeitlin, S. Guetersloh, L. Heilbronn, J. Miller, A. Fukumura, Y. Iwata, T. Murakami, L. Sihver, and D. Mancusi, "Fragmentation cross sections of medium-energy ^{35}Cl , ^{40}Ar , and ^{48}Ti beams on elemental targets," Phys. Rev. C **77** (2008) 034605; C. Zeitlin, A. Fukumura, S. B. Guetersloh, L. Heilbronn, Y. Iwata, J. Miller, and T. Murakami, "Fragmentation cross sections of ^{28}Si at beam energies from 290 to 120 A MeV," Nucl. Phys. **A784** (2007) 341–367; C. Zeitlin, L. Heilbronn, J. Miller, A. Fukumura, Y. Iwata, T. Murakami, J. MacGibbon, L. Pinsky, and T. Wilson, "Nuclear fragmentation cross sections for NASA database development," AIP Conf. Proc. **610** (2002) 285; C. Zeitlin, L. Heilbronn, J. Miller, S. E. Rademacher, T. Borak, T. R. Carter, K. A. Frankel, W. Schimmerling, and C. E. Stronach, "Heavy fragment production cross sections from 1.05 GeV/nucleon ^{56}Fe in C, Al, Cu, Pb, and CH_2 targets," Phys. Rev. C **56** (1997) 388–397.
Tabulated cross sections by *NASA Measurements Consortium: LBNL Cross-sections* are available on the LBNL group's website at: <http://fragserver.lbl.gov/main.html>.
- [18] J. W. Wilson, J. L. Shinn, L. W. Townsend, R. K. Tripathi, F. F. Badavi, and S. Y. Chun, "NUCFRG2: a semiempirical nuclear fragmentation model," Nucl. Instrum. Methods Phys. Res. B **94**, (1994) 95–102.
- [19] F. A. Cucinotta, J. W. Wilson, R. K. Tripathi, and L. W. Townsend, "Microscopic fragmentation model for galactic cosmic ray studies," Adv. Space Res. **22** (1998) 533–537.
- [20] B. S. Nilsen, C. J. Waddington, J. R. Cummings, T. L. Garrard, and J. Klarmann, "Fragmentation cross sections of relativistic $^{84}_{36}\text{Kr}$ and $^{109}_{47}\text{Ag}$ nuclei in targets from hydrogen to lead," Phys. Rev. C **52** (1995) 3277–3290.
- [21] C. Zeitlin, A. Fukumura, L. Heilbronn, Y. Iwata, J. Miller, and T. Murakami, "Fragmentation cross sections of 600 MeV/nucleon ^{20}Ne on elemental targets," Phys. Rev. C **64** (2001) 024902;
- [22] S. G. Mashnik, K. K. Gudima, N. V. Mokhov, and R. E. Prael, "LAQGSM03.03 Upgrade and Its Validation," LANL Research Note X-3-RN(U)07-15, August 27, 2007; LANL Report LA-UR-07-6198, E-print: arXiv:0709.173.
- [23] C. Zeitlin, S. Guetersloh, L. Heilbronn, J. Miller, A. Fukumura, Y. Iwata, and T. Murakami, "Fragmentation cross sections of 290 and 400 MeV/nucleon ^{12}C beams on elemental targets," Phys. Rev. C **76** (2007) 014911.
- [24] K. Sümerer and B. Blank, "Modified empirical parametrization of fragmentation cross sections," Phys. Rev. C **61** (2000) 034607.
- [25] H. Iwase, K. Niita, and T. Nakamura, "Development of General-Purpose Particle and Heavy Ion Transport Monte Carlo Code," J. Nucl. Sci. Technol. **39**, (2002) 1142–1151.

SGM:sgm

Distribution:

Eolus Team

B. J. Archer , X-3, F644

M. B. Chadwick, T-DO, B210

J. A. Carlson, T-2, B283

G. M. Hale, T-2, B214

A. J. Sierk, T-2, B214

R. C. Little, X-1-NAD, F663

J. D. Zumbro, X-1-TA, F663

L. S. Waters, D-5, K575

G. W. McKinney, D-5, K575

M. R. James, D-5, K575

E. J. Pitcher, LANSCE-DO, H816

M. J. Devlin, LANSCE-NS, H855

M. Mocko, LANSCE-LC H805

S. R. Elliott, P-23, H803

K. K. Kwiatkowski, P-23, H803

X-DO file

T-DO file

T-2 file

X-3 file